TARGETING OF GENE EXPRESSION TO THE TRABECULAR MESHWORK OF GLAUCOMATOUS BEAGLES BY NON-SELF-COMPLEMENTARY AAV2

By

Annie Oh

A THESIS

Submitted to
Michigan State University
in partial fulfillment of the requirement
for the degree of

Comparative Medicine and Integrative Biology- Master of Science

2014

ABSTRACT

TARGETING OF GENE EXPRESSION TO THE TRABECULAR MESHWORK OF GLAUCOMATOUS BEAGLES BY NON-SELF-COMPLEMENTARY AAV2

By

Annie Oh

Glaucoma is a leading cause of irreversible blindness in humans and dogs. Increased intraocular pressure (IOP) due to abnormal aqueous humor outflow through the trabecular meshwork (TM) is a major risk factor and is based on genetic predisposition. The purposes of these studies were to target gene expression to the canine TM and prevent or reverse IOP elevation in beagle dogs with inherited primary open angle glaucoma (POAG). In these animals, the disease is caused by a missense mutation in the *ADAMTS10* gene. Green fluorescent protein (GFP) reporter gene expression was successfully targeted to the conventional aqueous humor outflow pathway of *wild type* and *ADAMTS10*-mutant dogs using a non-self-complementary adeno-associated virus serotype 2 (AAV2) with a single capsid mutation: *AAV2(Y444F)-smCBA-GFP* (2×10^{10} vg/mL to 2×10^{12} vg/mL; 50 μL). The triple (Y444,500,730F) and quadruple (Y444,500,730F + T491V) mutant AAV2s were ineffective. Subsequent gene replacement therapy was performed in pre-glaucomatous (n=7) and glaucomatous (n=3) *ADAMTS10*-mutants with *AAV2(Y444F)-smCBA-hADAMTS10* at the highest dose (2×10^{12} vg/mL; 50 μL). The IOP of these animals were monitored weekly for 19 weeks. While the treatment was deemed safe with no severe adverse effects, a decrease in IOP was not observed. If the transgene was expressed, a therapeutic effect could probably be achieved by increasing the vector dose and number of transduced TM cells.

ACKNOWLEDGEMENTS

I would like to acknowledge and thank the many people that have helped me throughout the thesis process.

I first need to acknowledge my mentor, Dr. András Komáromy, for his unending support, patience, and kindness. He has always been a great inspiration and I can never thank him enough for all the great opportunities and fun-filled memories. I have learned so much and am truly grateful for having the chance to work with him.

To Dr. Simon Petersen-Jones and Dr. Joshua Bartoe for their generous support, mentorship, and knowledge that I will cherish throughout the course of my career. Dr. Vilma Yuzbasiyna-Gurkan, to whom I owe so much for her mentorship, knowledge, and enthusiasm during this process. Most importantly, for giving me the opportunity to pursue a Masters degree in the CMIB program. To my committee members, Dr. Sayoko Moroi, and Dr. Arthur Weber for their guidance, and input that has furthered my scientific development during my degree.

To the Hauswirth's and Boye's lab at the University of Florida, for their expertise in vector technology. To Dr. Gui-shuang Ying and Jiayan Huang at the University of Pennsylvania for their knowledge in biostatistics.

To everyone in the Komáromy lab – Christine Harman, and Kristin Koehl, for being great friends and fantastic teachers. Forrest Nussdorfer, Josh Laske, Ron Tsai, and Monica Choo, for their help during experiments, and of course, all the laughs and joyful memories. To the graduate students in Dr. Petersen-Jones's and Dr. Lorraine Sordillo's lab and the ophthalmology residents, particularly Dr. Laurence Occelli, for helping me with procedures, answering my

random questions, and being such a supportive friend during this process, and Dr. Connie Yeh, for all her kindness, advice, and fun nights out on the town.

Individuals at MSU - Lisa Allen and her staff for taking amazing care of the Vivarium dogs. And great thanks to Ramona for her enthusiasm and lovely smile. Dr. Victoria Hoelzer-Maddox for her administrative support that has helped me so much during my time at MSU. Dr. Melinda Frames at the Center for Advanced Microscopy for taking incredible images for the figures in the thesis.

Financial support from The Glaucoma Research Foundation, NIH Grants T32OD011167 (Michigan State University), EY021721 (University of Florida), and P30EY021721 (University of Florida), Research to Prevent Blindness (University of Florida), Foundation Fighting Blindness (University of Florida), and MSU Faculty Startup Funds.

To the Edward Sheppard and family for the unrestricted gift.

To my family, for all their love and to whom I owe everything.

Most importantly, to the Vivarium dogs that have sacrificed their lives for the advancement of science. Thank you and may you rest in peace in heaven.

TABLE OF CONTENTS

LIST OF TABLES

LIST OF FIGURES

KEY TO ABBREVIATIONS

Adeno-associated virus	AAV
Adeno-associated virus serotype 2	AAV2
Association for Research in Vision and Ophthalmology	ARVO
Balanced salt solution	BSS
Basic local alignment search tool	BLAST
Canine ADAMTS10	cADAMTS10
Confocal scanning laser ophthalmoscopy	cSLO
Cross-linked actin networks	CLAN
Extracellular matrix	ECM
Fibrillin-1	FBN1
Glycosaminoglycan	GAG
Generalized estimating equations	GEE
Human ADAMTS10	hADAMTS10
Human embryonic kidney 293 variant cells	HEK293T
Immunohistochemistry	IHC
Inferior-nasal	IN (AS2)
Inferior-temporal	IT (AS3)
Intraocular pressure	IOP
Inverted terminal repeat	IRT
Iridocorneal angle	ICA
Juxtacanalicular connective tissue	JCT

Marfan syndrome	MS
Matrix metalloprotease	MMP
Mega base pairs	Mb
Michigan State University	MSU
Myocilin	MYOC
Non-steroidal anti-inflammatory drug	NSAID
Optic nerve head	ONH
Optineurin	OPTN
Phosphate buffered saline	PBS
Primary open angle glaucoma	POAG
Retinal ganglion cell	RGC
Schlemm's canal	SC
Superior-nasal	SN (AS1)
Superior-temporal	ST (AS4)
Truncated hybrid chicken beta actin promoter	smCBA
Transforming growth factor-beta	TGF-β
Transforming growth factor-beta 2	TGF-β2
Tissue inhibitor of metalloprotease	TIMP
Trabecular meshwork	TM
Vector genome per milliliter	vg/mL
Weill-Marchesani syndrome	WMS
Wild type	*wt*

CHAPTER 1 - INTRODUCTION

Glaucoma is a common cause of blindness worldwide as an estimated 79.6 million people will be affected and 11.1 million people will be bilaterally blind by 2020.[1] The disease is defined as an optic neuropathy resulting in vision loss due to structural and functional injury to the optic nerve head (ONH) and retinal ganglion cells (RGCs).[2] Of the different types, primary open angle glaucoma (POAG) is the most prevalent form.[1] Unfortunately there is no cure, and lifelong monitoring and treatment is required in affected individuals.

POAG is a multifactorial disorder with a largely unknown pathogenesis.[3] Elevated intraocular pressure (IOP) is a major risk factor and the consequence of increased resistance to outflow at the trabecular meshwork (TM).[4, 5] Family history is another major risk factor as a confirmed first-degree relative raises the probability for an individual to develop POAG by ten times.[6] The disease does not follow a Mendelian inheritance pattern (single gene inheritance), and its onset and progression is influenced by multiple genes.[7] Traditional linkage analysis and genome wide association studies have identified several genes that are potentially coupled with POAG and/or IOP. The three well-established POAG genes are *MYOC*, *OPTN*, and *WDR36*.[3] *TMCO1* and *GAS7* are loci reported to be associated with regulating IOP.[8, 9] The discovery of novel genetic variants continues to expand the glaucoma genomic database, and paves the way for new diagnostics and treatments, such as DNA-based diagnostic testing, personalized medicine, and ocular gene therapy.[10]

Successful gene augmentation was previously demonstrated in *RPE65*-mutant dogs with an adeno-associated viral (AAV) vector.[11, 12] The methods were then translated to human clinical trials, which led to the restoration of vision in Leber Congenital Amaurosis type 2

patients.[13-17] Successful proof-of-concept therapies have also been demonstrated in canine models of achromatopsia,[18] and retinitis pigmentosa.[19-21] The results from these experiments have not only placed canines at the forefront of vision research, but exemplify the significant impact large animal models have in the field of translational medicine.

One of the best characterized and clinically relevant spontaneous animal models for POAG is the *ADAMTS10*-mutant beagle dog.[22,23] *ADAMTS10* encodes a metalloprotease that is highly expressed in the TM and involved in the formation of extracellular matrix (ECM). [24] The identification of the underlying G661R missense mutation in this causal gene provides a unique opportunity to study gene enhancement therapy. Therefore, the purpose of these experiments was to target gene expression with AAV to the canine TM and prevent or reverse IOP elevation in beagle dogs with inherited POAG. We hypothesize that introducing the *wt ADAMTS10* cDNA to the TM will rescue the POAG disease phenotype. The significance of our study was to establish the groundwork for TM-directed gene therapy in a large animal model.

REFERENCES

REFERENCES

1. Quigley HA, Broman AT. The number of people with glaucoma worldwide in 2010 and 2020. *The British Journal of Ophthalmology* 2006;90:262-267.

2. Foster PJ, Buhrmann R, Quigley HA, Johnson GJ. The definition and classification of glaucoma in prevalence surveys. *The British Journal of Ophthalmology* 2002;86:238-242.

3. Gemenetzi M, Yang Y, Lotery AJ. Current concepts on primary open-angle glaucoma genetics: a contribution to disease pathophysiology and future treatment. *Eye* 2012;26:355-369.

4. Quigley HA. Glaucoma. *Lancet* 2011;377:1367-1377.

5. Coleman AL, Miglior S. Risk factors for glaucoma onset and progression. *Survey of Ophthalmology* 2008;53 Suppl1:S3-10.

6. Wolfs RC, Klaver CC, Ramrattan RS, van Duijn CM, Hofman A, de Jong PT. Genetic risk of primary open-angle glaucoma. Population-based familial aggregation study. *Archives of Ophthalmology* 1998;116:1640-1645.

7. Wiggs JL. Genetic etiologies of glaucoma. *Archives of Ophthalmology* 2007;125:30-37.

8. van Koolwijk LM, Ramdas WD, Ikram MK, et al. Common genetic determinants of intraocular pressure and primary open-angle glaucoma. *PLoS Genetics* 2012;8:e1002611.

9. Ozel AB, Moroi SE, Reed DM, et al. Genome-wide association study and meta-analysis of intraocular pressure. *Human Genetics* 2014;133:41-57.

10. Moroi SE, Raoof DA, Reed DM, Zollner S, Qin Z, Richards JE. Progress toward personalized medicine for glaucoma. *Expert Review of Ophthalmology* 2009;4:145-161.

11. Acland GM, Aguirre GD, Ray J, et al. Gene therapy restores vision in a canine model of childhood blindness. *Nature Genetics* 2001;28:92-95.

12. Narfstrom K, Katz ML, Bragadottir R, et al. Functional and structural recovery of the retina after gene therapy in the RPE65 null mutation dog. *Investigative Ophthalmology & Visual Science* 2003;44:1663-1672.

13. Bainbridge JW, Smith AJ, Barker SS, et al. Effect of gene therapy on visual function of Leber's congenital amaurosis. *The New England Journal of Medicine* 2008;358:2231-2239.

14. Maguire AM, Simonelli F, Pierce EA, et al. Safety and efficacy of gene transfer for Leber's congenital amaurosis. *The New England Journal of Medicine* 2008;358:2240-2248.

15. Hauswirth WW, Aleman TS, Kaushal S, et al. Treatment of leber congenital amaurosis due to RPE65 mutations by ocular subretinal injection of adeno-associated virus gene vector: short-term results of a phase I trial. *Human Gene Therapy* 2008;19:979-990.

16. Simonelli F, Maguire AM, Testa F, et al. Gene therapy for Leber's congenital amaurosis is safe and effective through 1.5 years after vector administration. *Molecular Therapy: The Journal of the American Society of Gene Therapy* 2010;18:643-650.

17. Jacobson SG, Cideciyan AV, Ratnakaram R, et al. Gene therapy for leber congenital amaurosis caused by RPE65 mutations: safety and efficacy in 15 children and adults followed up to 3 years. *Archives of Ophthalmology* 2012;130:9-24.

18. Komaromy AM, Alexander JJ, Rowlan JS, et al. Gene therapy rescues cone function in congenital achromatopsia. *Human Molecular Genetics* 2010;19:2581-2593.

19. Beltran WA, Cideciyan AV, Lewin AS, et al. Gene therapy rescues photoreceptor blindness in dogs and paves the way for treating human X-linked retinitis pigmentosa. *Proceedings of the National Academy of Sciences of the United States of America* 2012;109:2132-2137.

20. Lheriteau E, Petit L, Weber M, et al. Successful gene therapy in the RPGRIP1-deficient dog: a large model of cone-rod dystrophy. *Molecular Therapy: The Journal of the American Society of Gene Therapy* 2014;22:265-277.

21. Petit L, Lheriteau E, Weber M, et al. Restoration of vision in the pde6beta-deficient dog, a large animal model of rod-cone dystrophy. *Molecular Therapy: The Journal of the American Society of Gene Therapy* 2012;20:2019-2030.

22. Gelatt KN, Gilger BC, Kern TJ. *Veterinary Ophthalmology*. 5th ed. Ames, Iowa: Wiley-Blackwell; 2013.

23. Kuchtey J, Olson LM, Rinkoski T, et al. Mapping of the disease locus and identification of ADAMTS10 as a candidate gene in a canine model of primary open angle glaucoma. *PLoS Genetics* 2011;7:e1001306.

24. Apte SS. A disintegrin-like and metalloprotease (reprolysin-type) with thrombospondin type 1 motif (ADAMTS) superfamily: functions and mechanisms. *The Journal of Biological Chemistry* 2009;284:31493-31497.

CHAPTER 2 - LITERATURE SURVEY

Aqueous humor dynamics

The ciliary body is an anterior continuation of the choroid and is topographically divided into two regions: the anterior pars plicata and posterior pars plana.[1] Ciliary processes in the pars plicata produce aqueous humor through diffusion, ultrafiltration, and active secretion of solutes. Diffusion occurs down a concentration gradient across cell membranes, and ultrafiltration encompasses hydrostatic pressures that force water and water-soluble substances across the fenestrated ciliary capillary endothelium. These two passive mechanisms create a 'reservoir' of plasma ultrafiltrate in the ciliary stroma. Certain ions and substances are then actively secreted across the nonpigmented ciliary epithelium into the posterior chamber to form aqueous humor. The Na+/K+ ATPase complex and carbonic anhydrase are two enzymes associated with the active transport of solutes and are responsible for 80-90% of total fluid formation.[2]

Once generated, aqueous humor travels from the posterior chamber to the anterior chamber, providing nutrients and removing waste products for the avascular lens and cornea. It finally exits the eye through the trabecular and uveoscleral outflow pathways of the ICA.[1] In the healthy eye, moderate aqueous outflow resistance in the ICA is required to generate IOP (10-20 mm Hg) for proper maintenance of globe shape and optics for vision. Thus, tightly controlled aqueous humor production and outflow drainage are important processes for normal ocular function.[2]

Aqueous humor outflow pathways

The main route for aqueous humor exit is through the conventional or trabecular outflow pathway. In humans, this route is comprised of the TM, Schlemm's canal (SC), collector

channels, and aqueous veins that lead into the episcleral venous system.[3] The SC is a single circular structure that collects aqueous humor before it enters the bloodstream. A minor pathway (4-14%) also exists, called the unconventional or uveoscleral outflow pathway. Fluid flows through the ciliary muscle bundles to the suprachoroidal space before diffusing across the sclera into the intrascleral venous system.[4] The canine conventional pathway (Figure 2.1) is different because pectinate ligaments secure the iris to the limbal cornea, and instead of having a SC, the dog possesses multiple vessels collectively known as the angular aqueous venous plexus.[5] The canine uveoscleral pathway is similar to humans, and is responsible for ~15% of total aqueous humor outflow.[1]

The TM is critical in the regulation of aqueous humor outflow resistance and generation of IOP. In humans, it is located in the anterior region of the ICA at the scleral sulcus and consists of three areas, the uveal meshwork, corneoscleral meshwork, and juxtacanalicular tissue (JCT).[3] The uveal and corneoscleral meshworks are organized and comprised of fenestrated trabecular beams with large intertrabecular spaces between adjacent sheets.[6] In contrast, the JCT does not form trabecular beams and is mainly composed of a loose network of extracellular matrix (ECM).[7] All three regions are embedded with TM cells that protrude fibroblastlike processes, and communicate with adjacent cells and those of the inner endothelium of the SC. These cells also exhibit phagocytic properties that may act to remove cellular debris.[3] The inner endothelial wall of the SC forms giant vacuoles with intra- and paracellular pores which open into the lumen in response to pressure from aqueous humor flow. These pores control fluid flow and generate up to10% of the total resistance in normal human eyes depending on the number of pores present in the inner wall.[8, 9]

Figure 2.1: Hybrid aqueous outflow pathways of humans and dogs. The aqueous humor outflow pathways in the dog have two main distinctive structures: the pectinate ligaments and the aqueous venous plexus.

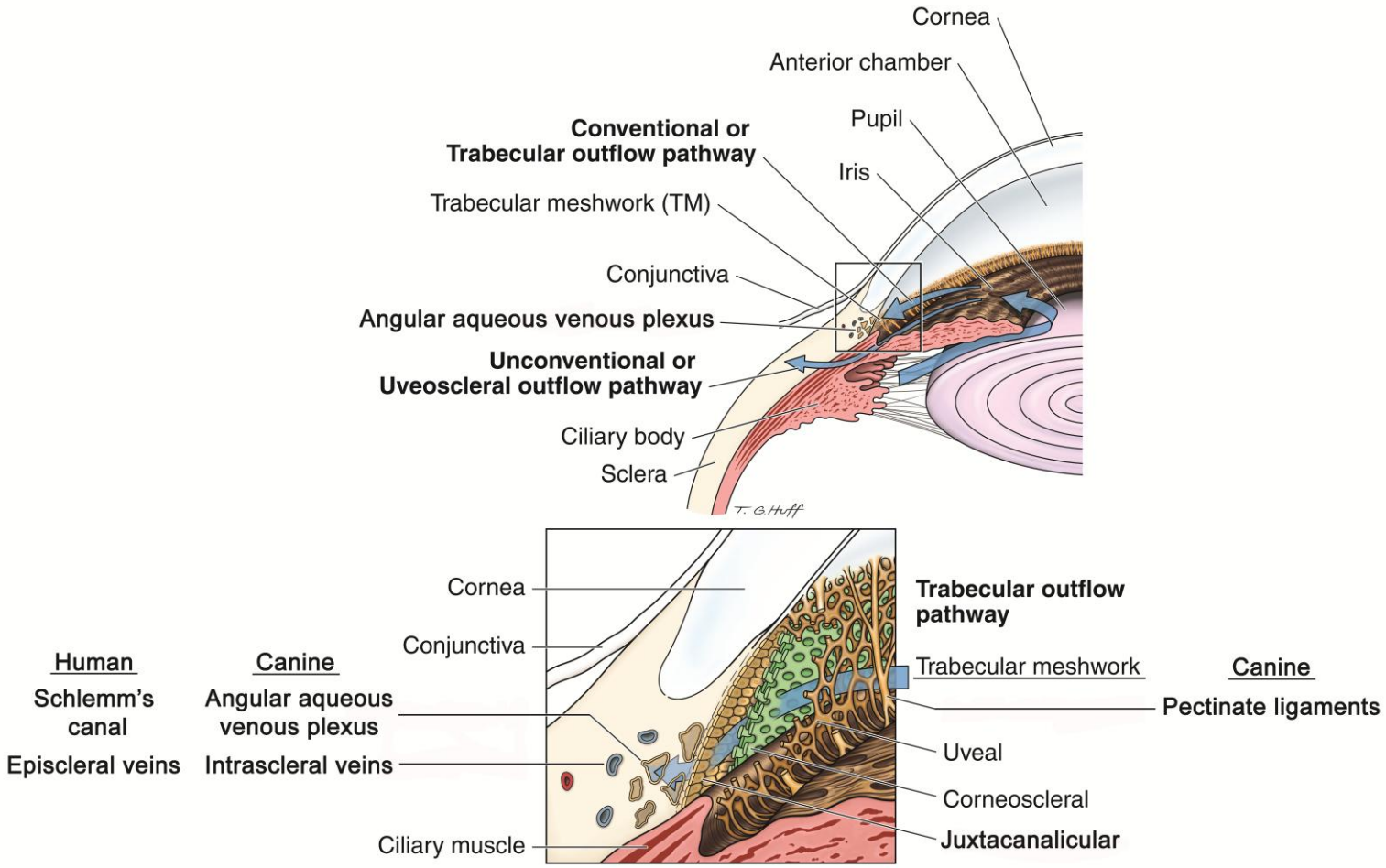

In canines, the TM is located in the posterior region of the ICA within the ciliary cleft. The tissue structures of the canine TM outflow pathway, analyzed by transmission and scanning electron microscopy, are similar to the humans' as describe above.[1, 5, 10]

Extracellular matrix turnover and outflow resistance

The precise location of aqueous humor outflow resistance in normal and glaucomatous eyes is still under debate.[11] It is widely hypothesized that the bulk of resistance in both normal and glaucomatous eyes occurs in the JCT of the TM; a region that is highly dynamic and undergoes constant remodeling. Normal homeostatic adjustments of outflow resistance appears to be triggered by embedded TM cells that sense mechanical stretch from IOP and respond by secreting matrix metalloproteases (MMPs).[12] Studies with mechanical stretching models *in vitro* have shown an increase in MMP1, 2, 3, 9, and 14.[12, 13] These enzymes selectively breakdown ECM components including proteoglycans, laminin, fibronectin, collagens (type IV and type VI), elastin, and osteonectin[7] contributing to the expansion of the JCT and thereby permitting increased aqueous humor outflow.[14] Additional proteinases, such as ADAM, ADAMTS, and tissue plasminogen activator, also play possible roles in modulating outflow resistance.[13]

Normal ECM homeostasis is tightly controlled by enzymes such as tissue inhibitor metalloproteases (TIMPs).[13] However, reduced or disorganized ECM turnover rate may lead to increased aqueous humor outflow resistance as seen in POAG. Abnormal ECM remodeling mainly results in an accumulation of excess material and fibrosis of the TM.[6] These accumulations are normally present in older individuals, but there is a significantly greater amount of fibrosis and certain components, such as proteoglycans, in the glaucomatous TM.[15]

Transforming growth factor beta 2 (TGF-β2) is a profibrotic cytokine that is normally secreted into aqueous humor by TM cells, ciliary body epithelium, and the lens, to promote ocular immune privilege.[16-18] In glaucomatous patients, excessive levels of this cytokine have been consistently identified.[19] Studies with human TM cells in monolayer cell cultures revealed that exogenous perfusion of TGF-β2 leads to the increased synthesis and expression of a broad variety of proteins, including collagens, elastin, fibronectin, laminin, and myocilin, in addition to plasminogen activator inhibitor (PAI-1), which inhibits MMPs.[16] It also induces the synthesis of ECM cross-linking enzymes such as tissue transglutaminase (TGM2), lysyl oxidase (LOX), and lysyl oxidase-like proteins.[17] Furthermore, anterior eye segment perfusion culture models treated with TGF-β2 revealed a measurable decrease in fluid outflow resulting in increased IOP.[20] Therefore, excess TGF-β2 may be linked to the pathogenesis of POAG.

Glucocorticoids (GCs) have also been shown to disorganize ECM degradation. Administration of GCs results in ocular hypertension in approximately 40% of the general human population.[21] These 'steroid responders' are likewise more prone to develop POAG compared to nonresponders. Studies have shown that GCs inhibit TM cell phagocytosis, MMP activity, and subsequently increase the production of fibrillar proteins. Perfusion of human anterior segments also demonstrated that GCs gradually remodel TM cytoskeleton to form cross-linked actin networks (CLANs). The purpose of the CLANs in the outflow pathway is still unknown, but the unusual arrangement may block aqueous humor outflow.[22]

Animal models of glaucoma

In vitro and *in vivo* studies are crucial in understanding the fundamental aspects of human glaucoma. In particular, *in vivo* experiments in animal models have become the key medium for translational research.[23] Several large and small species have been categorized as spontaneous, induced, or transgenic models of glaucoma (Table 2.1 examples). In spontaneous models, the disease is inherited or occurs naturally.[24] In induced and transgenic models, the animals' anatomic structures or genome are altered to exhibit glaucomatous phenotypes.[25] In the end, all glaucoma models aim to simulate elevated and sustained IOP, and/or RGC loss.

There are advantages and disadvantages to every animal model. For example, nonhuman primates have a well-developed SC, lamina cribrosa, peripapillary sclera and blood supply that is virtually identical to the humans.[26] Unfortunately, nonhuman primates may not be practical for many research groups because they are expensive, have limited availability, hard to handle, and require an experienced staff in addition to special housing facilities.[27] Even though a colony of rhesus monkeys was previously described to exhibit spontaneous POAG,[28] there is currently no natural disease model available in nonhuman primates.

The mouse is simple to upkeep, produces large colonies, and has a SC.[27, 29] Since their genomes are thoroughly mapped and easy to manipulate, they have been essential in understanding the outcomes of *wild type (wt)* and mutant gene products.[23] However, a disadvantage of the mouse is the size of their eyes, and the poorly developed lamina cribrosa which lacks choroidal vascular supply.[30] Depending on the question at hand, different animal models provide the tools required for a greater understanding of glaucoma.

Table 2.1: Examples of glaucoma animal models.

Species	Size	Model mode	Method	References
Monkey	Large	Spontaneous	Inherited	[26]
		Induced	Laser photocoagulation of TM	[64]
		Induced	Intracameral injection of latex microspheres	[65]
Dog	Large	Spontaneous	Inherited	[34, 51]
Cat	Large	Spontaneous	Inherited	
Sheep and cow	Large	Induced	Application of glucocorticoids	[66, 67]
Mice	Small	Transgenic	*MYOC* mutation	[68]
		Transgenic	*OPTN* mutation	[69]
		Transgenic	α1 subunit of collagen Type 1 mutation	[70]
Rabbit	Small	Induced	Application of glucocorticoids	[71]
Zebrafish	Small	Transgenic	*Lrp2* mutation	[72]

TM: trabecular meshwork; *MYOC:* myocilin*; OPTN:* optineurin*; Lrp2*: low-density lipoprotein-related protein 2

Primary open angle glaucoma in beagle dogs

Among all animal species studied, dogs have the highest prevalence of primary glaucoma comparable to the disease frequency in humans. The highest frequency of primary glaucomas are found in purebred dogs (0.89%) with twenty-two breeds (Table 2.2), including the American Cocker Spaniel (5.52%), Bassett Hound (5.44%), and Chow Chow (4.70%), having a prevalence greater than 1%.[31] Contrary to the human glaucomas, the closed-angle form occurs more frequently in the general canine population, while the open angle form is considered to be rare.[32] Thanks to a colony of dogs maintained for ~40 years at the University of Florida, POAG in beagle dogs is one of the best studied and well-established natural/spontaneous animal models for glaucoma.[33] It is an autosomal recessive disorder caused by a missense mutation in *ADAMTS10,*[34, 35] and has a predictable onset with severe glaucomatous changes occurring later in life.[36] The slow and progressive nature of the disease provides windows of opportunity for various biochemical and morphologic research.[24] Beagle dogs with inherited POAG are also a valuable animal model because they share many phenotypic characteristics with the human form.[1] Furthermore, the dogs' eye size and ocular anatomy make them excellent subjects for clinical studies.[27]

Early studies have defined three stages of the disease: early (8-16 months), moderate (13-30 months), and advanced (2-4 years).[37] At 8-16 months of age, pressures begin to rise from the normal range of 10-20 mmHg, and by 2-4 years, the mean IOPs range from 25-40 mmHg. Notably, the ICA of POAG beagle dogs is open until the late disease stages.[38]

Table 2.2: Top breeds with high prevalence of primary glaucoma (1994 – 2002).[29]

Breed	**% Affected**
Overall	0.89%
American Cocker Spaniel	5.52%
Bassett Hound	5.44%
Chow Chow	4.70%
Shar-Pei	4.40%
Boston Terrier	2.88%
Fox Terrier, Wire	2.28%
Norwegian Elkhound	1.98%
Siberian Husky	1.88%
Cairn Terrier	1.82%
Poodle, Miniature	1.68%
Samoyed	1.59%
Bichon Frise	1.59%
Shih Tzu	1.58%
Australian Cattle Dog	1.51%
Akita	1.39%
Jack Russell Terrier	1.37%
English Cocker Spaniel	1.35%
Lhasa Apso	1.33%
Bouvier des Flandres	1.31%
Pekingese	1.22%
Poodle, Toy	1.20%
Beagle	1.10%

Analogous to the human form, the exact source of increased aqueous humor outflow resistance is still unknown. Transmission electron microscopy of normal and affected eyes revealed a fully differentiated ICA devoid of developmentally abnormalities at 3 months of age.[10] However at 12 months, clustering of fibrils and irregular elastic fibers were observed, and extracellular debris, such as glycosaminoglycan-like hyaluronidase-resistant material, start to appear in the TM.[39] Increased amounts of myocilin have also been localized to this region, and aqueous humor levels are increased in glaucomatous dogs.[40, 41] The role of myocilin is unknown, but mutations in this gene account for 3% of human POAG and the variant protein is hypothesized to decrease aqueous humor outflow facility.[42] In glaucomatous dogs, aqueous humor outflow facility, measured by pneumotonography, gradually decreases from 0.19 ± 0.07 μL/min/mmHg at 3-6 months of age to 0.07 ± 0.05 μL/min/mmHg at 43-48 months of age.[1] In the final stages of the disease, the trabeculae are compressed and disorganized, and the ICA is clinically narrowed and occasionally closed.[10] Consequently, sustained elevated IOP is the main cause of damage in these animals.

Another feature of glaucoma in beagles is lens zonule pathology. Early in the disease, stretching and tears of the lens zonules is observed at maximum mydriasis (dilation of the pupil).[43] As the IOP continues to rise, progressive focal disinsertion of these structures leads to subluxation of the lens and prolapse of the vitreous humor into the anterior chamber.[37] Increased pressures also results in an enlargement of the globe.[1] Posterior structures of the eye, specifically the ONH and RGCs, are also severely affected. In dogs, the normal ONH slightly protrudes into the vitreous chamber due to myelination of nerve fibers prior to the lamina cribrosa,[44] and at 5-6 months of age there is no noteworthy difference between normal and pre-glaucomatous individuals.[45] With progressive elevations in pressure, variable loss of RGC axons and myelin,

in addition to the posterior displacement of the lamina cribrosa, results in ONH atrophy and cupping. [36, 37, 46] Along with demyelination, the mechanical impact on RGC axons results in reduced axoplasmic flow.[46, 47] Consequently, the excessive release of excitotoxic amino acid glutamate by dying RGCs is suspected to cause further injury and death to neighboring cells.[48]

ADAMTS10 gene

ADAMTS10 is part of a superfamily of secreted proteases involved in the formation of ECM.[49] A G661R missense mutation in *ADAMTS10* was identified as the cause for beagle POAG. While the exact molecular mechanism still needs to be determined, the gene is highly expressed in the TM, and the mutation results in a misfolded protein that may be responsible for the excessive accumulation of ECM material in the TM of affected dogs.[34] Following these results, the 'Microfibril hypothesis of glaucoma' was proposed which postulates that genetic mutations in microfibril-associated genes, including *Fibrillin-1 (FBN1)* and *ADAMTS10*, lead to altered connective tissue integrity. The abnormal connective tissue integrity results in dysregulation of growth factors signaling, most notably TGF-β2.[50]

In man, mutations in *ADAMTS10* as well as related genes *ADAMTS17* and *FBN1* involved in microfibril metabolism are responsible for diseases such as Weill-Marchesani syndrome (WMS) and Marfan syndrome (MS). These inherited connective tissue disorders are characterized by skeletal abnormalities including brachydactyly in WMS and arachnodactyly in MS. The ocular phenotypes of both syndromes include ectopia lentis and glaucoma.[51] Ectopia lentis is likely due to mutated FBN1 and ADAMTS10 proteins, which are required for lens zonule formation and maintenance.[51, 52] FBN1 is a major component of lens zonule microfibrils and ADAMTS10 protein accelerates FBN1 microfibril formation in fibroblast culture.[53] The

glaucoma phenotype is different between WMS and MS. In WMS, the lens may subluxate into the pupil or anterior chamber and cause secondary acute angle closure glaucoma.[51] In contrast, the lens tends to subluxate posteriorly in MS, and the glaucoma phenotype is an open-angle.[54]

Interestingly in dogs, there is no systemic phenotype seen with *ADAMTS10* and *ADAMTS17* mutations. While the variant ADAMTS17 described in terrier breeds results in primary lens-luxation with secondary glaucoma,[55] the predominant clinical sign in *ADAMTS10*-mutant beagles is POAG. Lens zonule dysplasia is also reported in the beagles[43], but is less prominent compared to POAG. TGF-β2 levels are elevated in aqueous humor of human patients with POAG.[19] However, an increased concentration of this profibrotic cytokine has not yet been reported in the eyes of mutant beagle dogs. Nevertheless, abnormal microfibril homeostasis in the TM and dysregulation of TGF-β2 seems to be highly linked to the pathogenesis of POAG in both humans and dogs.[50]

Viral vectors of gene therapy

The current treatment of glaucoma consists of slowing the disease progression by lowering IOP through medical and/or surgical means. In canines, short-term IOP control includes the administration of a single, or combination of drugs, while long-term control involves the use of several medications to supplement surgical procedures, such as cyclophotocoagulation. The most commonly used topical ophthalmic solutions in clinics are dorzolamide (carbonic anhydrase inhibitor), timolol maleate (beta blocker), and latanoprost (prostaglandin analog).[1]

Viral mediated gene therapy is a potential treatment option. Since a loss of function mutation in *ADAMTS10* has been identified as the cause for POAG in beagle dogs, this animal serves as a spontaneous model to determine if TM-targeted gene replacement therapy can rescue

the POAG disease phenotype. Currently, the three most commonly studied viral vectors in basic science and translational research are adenovirus, lentivirus, and AAV, each possessing their own major advantages and disadvantages.[56]

Compared to the others, AAV is the most commonly used viral vector for ocular gene therapy.[56] It is a single-stranded DNA parvovirus that infects both nondividing and dividing cells, and produces persistent transgene expression. More importantly, AAV is an attractive delivery vehicle because it is non-replicating and elicits a benign immune response making it safe to use in preclinical and clinical trials. The main disadvantage is that researchers can only package a small amount of genetic material (~5kb) into the icosahedral, non-enveloped capsid.[57, 58]

The variety of serotypes and their transgenes has enhanced AAV's potential as a therapy vector. Twelve human serotypes (AAV1-12) have been described, each exhibiting particular tropisms.[59] Natural variations in the amino acid sequences of the three proteins capsids, VP1, VP2, and VP3, dictates the virus' serotype and affinity for certain tissues. AAV's genome codes inverted terminal repeats (IRTs) that are responsible for packaging genomic data into capsids. Replacing the *wt* region between the IRTs produces recombinant AAV that can deliver a DNA sequence of interest.[60, 61]

Innovations in vector technology have further improved cell tropism, efficiency of transduction, and transgene expression intensity. Hybrid vectors have enhanced cell-specific targeting by packaging the serotype 2 into the capsid of other AAVs, such as serotype 5 (AAV2/5).[62] Self-complementary constructs result in more robust transgene expression by eluding DNA second strand synthesis, a rate limiting step for AAV transduction.[63, 64] Mutations of AAV capsid tyrosine threonine residues also elicit improved viral vector nuclear transport and

a stronger transgene expression by avoiding phosphorylation and ubiquitination of exposed tyrosine residues and subsequent proteasome-mediated degradation.[65] These modifications have expanded the realm of AAV targetable ocular tissues and inherited diseases.

REFERENCES

REFERENCES

1. Gelatt KN, Gilger BC, Kern TJ. *Veterinary Ophthalmology*. 5th ed. Ames, Iowa: Wiley-Blackwell; 2013.

2. Goel M, Picciani RG, Lee RK, Bhattacharya SK. Aqueous humor dynamics: a review. *The Open Ophthalmology Journal* 2010;4:52-59.

3. Tamm ER. The trabecular meshwork outflow pathways: structural and functional aspects. *Experimental Eye Research* 2009;88:648-655.

4. Alm A, Nilsson SF. Uveoscleral outflow--a review. *Experimental Eye Research* 2009;88:760-768.

5. Samuelson DA. A Reevaluation of the Comparative Anatomy of the Eutherian Iridocorneal Angle and Associated Ciliary Body Musculature. *Veterinary & Comparative Ophthalmology* 1996;6:153-171.

6. Keller KE, Acott TS. The Juxtacanalicular Region of Ocular Trabecular Meshwork: A Tissue with a Unique Extracellular Matrix and Specialized Function. *Journal of Ocular Biology* 2013;1:3.

7. Acott TS, Kelley MJ. Extracellular matrix in the trabecular meshwork. *Experimental Eye Research* 2008;86:543-561.

8. Johnson M, Shapiro A, Ethier CR, Kamm RD. Modulation of outflow resistance by the pores of the inner wall endothelium. *Investigative Ophthalmology & Visual Science* 1992;33:1670-1675.

9. Bill A, Svedbergh B. Scanning electron microscopic studies of the trabecular meshwork and the canal of schlemm-an attempt to localize the main resistance to outflow of aqueous humor in man. *Acta Ophthalmologica* 1972;295-320.

10. Samuelson DA, Gum GG, Gelatt KN. Ultrastructural changes in the aqueous outflow apparatus of beagles with inherited glaucoma. *Investigative Ophthalmology & Visual Science* 1989;30:550-561.

11. Johnson M. 'What controls aqueous humour outflow resistance?'. *Experimental Eye Research* 2006;82:545-557.

12. Bradley JM, Kelley MJ, Zhu X, Anderssohn AM, Alexander JP, Acott TS. Effects of mechanical stretching on trabecular matrix metalloproteinases. *Investigative Ophthalmology & Visual Science* 2001;42:1505-1513.

13. Keller KE, Aga M, Bradley JM, Kelley MJ, Acott TS. Extracellular matrix turnover and outflow resistance. *Experimental Eye Research* 2009;88:676-682.

14. Alexander JP, Samples JR, Van Buskirk EM, Acott TS. Expression of matrix metalloproteinases and inhibitor by human trabecular meshwork. *Investigative Ophthalmology & Visual Science* 1991;32:172-180.

15. Tektas OY, Lutjen-Drecoll E. Structural changes of the trabecular meshwork in different kinds of glaucoma. *Experimental Eye Research* 2009;88:769-775.

16. Fuchshofer R, Tamm ER. Modulation of extracellular matrix turnover in the trabecular meshwork. *Experimental Eye Research* 2009;88:683-688.

17. Wordinger RJ, Sharma T, Clark AF. The role of TGF-beta2 and bone morphogenetic proteins in the trabecular meshwork and glaucoma. *Journal of Ocular Pharmacology and Therapeutics: The Official Journal of the Association for Ocular Pharmacology and Therapeutics* 2014;30:154-162.

18. Streilein JW. Ocular immune privilege: therapeutic opportunities from an experiment of nature. *Nature Reviews Immunology* 2003;3:879-889.

19. Inatani M, Tanihara H, Katsuta H, Honjo M, Kido N, Honda Y. Transforming growth factor-beta 2 levels in aqueous humor of glaucomatous eyes. *Graefe's Archive for Clinical and Experimental Ophthalmology = Albrecht von Graefes Archiv fur Klinische und Experimentelle Ophthalmologie* 2001;239:109-113.

20. Fleenor DL, Shepard AR, Hellberg PE, Jacobson N, Pang IH, Clark AF. TGFbeta2-induced changes in human trabecular meshwork: implications for intraocular pressure. *Investigative Ophthalmology & Visual Science* 2006;47:226-234.

21. Clark AF, Wordinger RJ. The role of steroids in outflow resistance. *Experimental Eye Research* 2009;88:752-759.

22. Clark AF, Brotchie D, Read AT, et al. Dexamethasone alters F-actin architecture and promotes cross-linked actin network formation in human trabecular meshwork tissue. *Cell Motility and the Cytoskeleton* 2005;60:83-95.

23. Zeiss CJ. Translational models of ocular disease. *Veterinary Ophthalmology* 2013;16 Suppl 1:15-33.

24. Gelatt KN, Brooks DE, Samuelson DA. Comparative glaucomatology. I: The spontaneous glaucomas. *Journal of Glaucoma* 1998;7:187-201.

25. Gelatt KN, Brooks DE, Samuelson DA. Comparative glaucomatology. II: The experimental glaucomas. *Journal of Glaucoma* 1998;7:282-294.

26. Morrison JC, Cepurna Ying Guo WO, Johnson EC. Pathophysiology of human glaucomatous optic nerve damage: insights from rodent models of glaucoma. *Experimental Eye Research* 2011;93:156-164.

27. Bouhenni RA, Dunmire J, Sewell A, Edward DP. Animal models of glaucoma. *J Biomed Biotechnol* 2012;2012:692609.

28. Dawson WW, Brooks DE, Hope GM, et al. Primary open angle glaucomas in the rhesus monkey. *The British Journal of Ophthalmology* 1993;77:302-310.

29. Rodriguez-Ramos Fernandez J, Dubielzig RR. Ocular comparative anatomy of the family Rodentia. *Veterinary Ophthalmology* 2013;16 Suppl 1:94-99.

30. May CA, Lutjen-Drecoll E. Morphology of the murine optic nerve. *Investigative Ophthalmology & Visual Science* 2002;43:2206-2212.

31. Gelatt KN, MacKay EO. Prevalence of the breed-related glaucomas in pure-bred dogs in North America. *Veterinary Ophthalmology* 2004;7:97-111.

32. Maggs DJ, Miller PE, Ofri R, Slatter DH. *Slatter's Fundamentals of Veterinary Ophthalmology*. 5th ed. St. Louis, Mo.: Elsevier; 2013:x, 506 p.

33. Gelatt KN. Familial glaucoma in the Beagle dog. *Journal of the American Animal Hospital Association* 1972;23-28.

34. Kuchtey J, Olson LM, Rinkoski T, et al. Mapping of the disease locus and identification of ADAMTS10 as a candidate gene in a canine model of primary open angle glaucoma. *PLoS Genetics* 2011;7:e1001306.

35. Kuchtey J, Kunkel J, Esson D, et al. Screening ADAMTS10 in dog populations supports Gly661Arg as the glaucoma-causing variant in beagles. *Investigative Ophthalmology & Visual Science* 2013;54:1881-1886.

36. Gelatt KN, Gum GG. Inheritance of primary glaucoma in the beagle. *American Journal of Veterinary Research* 1981;42:1691-1693.

37. Gelatt KN, Peiffer RL, Jr., Gwin RM, Gum GG, Williams LW. Clinical manifestations of inherited glaucoma in the beagle. *Investigative Ophthalmology & Visual Science* 1977;16:1135-1142.

38. Gelatt KN, Gum GG, Gwin RM, Bromberg NM, Merideth RE, Samuelson DA. Primary open angle glaucoma: inherited primary open angle glaucoma in the beagle. *The American Journal of Pathology* 1981;102:292-295.

39. Gum GG, Samuelson DA, Gelatt KN. Effect of hyaluronidase on aqueous outflow resistance in normotensive and glaucomatous eyes of dogs. *American Journal of Veterinary Research* 1992;53:767-770.

40. Hart H, Samuelson DA, Tajwar H, et al. Immunolocalization of myocilin protein in the anterior eye of normal and primary open-angle glaucomatous dogs. *Veterinary Ophthalmology* 2007;10 Suppl 1:28-37.

41. Mackay EO, Kallberg ME, Gelatt KN. Aqueous humor myocilin protein levels in normal, genetic carriers, and glaucoma Beagles. *Veterinary Ophthalmology* 2008;11:177-185.

42. Borras T. The effects of myocilin expression on functionally relevant trabecular meshwork genes: a mini-review. *Journal of Ocular Pharmacology and Therapeutics: The Official Journal of the Association for Ocular Pharmacology and Therapeutics* 2014;30:202-212.

43. Teixeira L, Scott E, Iwabe S, Dubielzig RR, Komaromy A. Zonular ligament dysplasia in beagles with hereditary primary open angle glaucoma (POAG). ARVO Meeting; 2013.

44. Brooks DE, Komaromy AM, Kallberg ME. Comparative retinal ganglion cell and optic nerve morphology. *Veterinary Ophthalmology* 1999;2:3-11.

45. Palko JR, Iwabe S, Pan X, Agarwal G, Komaromy AM, Liu J. Biomechanical properties and correlation with collagen solubility profile in the posterior sclera of canine eyes with an ADAMTS10 mutation. *Investigative Ophthalmology & Visual Science* 2013;54:2685-2695.

46. Brooks DE, Samuelson DA, Gelatt KN, Smith PJ. Morphologic changes in the lamina cribrosa of beagles with primary open-angle glaucoma. *American Journal of Veterinary Research* 1989;50:936-941.

47. Samuelson DA, Williams L, Gelatt KN, Gum GG, Meredith R. Orthograde rapid axoplasmic transport and ultrastructural changes of the optic nerve. Part II. Beagles with primary open-angle glaucoma. *Glaucoma* 1983;174-184.

48. Brooks DE, Garcia GA, Dreyer EB, Zurakowski D, Franco-Bourland RE. Vitreous body glutamate concentration in dogs with glaucoma. *American Journal of Veterinary Research* 1997;58:864-867.

49. Apte SS. A disintegrin-like and metalloprotease (reprolysin-type) with thrombospondin type 1 motif (ADAMTS) superfamily: functions and mechanisms. *The Journal of Biological Chemistry* 2009;284:31493-31497.

50. Kuchtey J, Kuchtey RW. The microfibril hypothesis of glaucoma: implications for treatment of elevated intraocular pressure. *Journal of Ocular pPharmacology and Therapeutics: The Official Journal of the Association for Ocular Pharmacology and Therapeutics* 2014;30:170-180.

51. Hubmacher D, Apte SS. Genetic and functional linkage between ADAMTS superfamily proteins and fibrillin-1: a novel mechanism influencing microfibril assembly and function. *Cellular and Molecular Life Sciences: CMLS* 2011;68:3137-3148.

52. Cain SA, Morgan A, Sherratt MJ, Ball SG, Shuttleworth CA, Kielty CM. Proteomic analysis of fibrillin-rich microfibrils. *Proteomics* 2006;6:111-122.

53. Kutz WE, Wang LW, Bader HL, et al. ADAMTS10 protein interacts with fibrillin-1 and promotes its deposition in extracellular matrix of cultured fibroblasts. *The Journal of Biological Chemistry* 2011;286:17156-17167.

54. Izquierdo NJ, Traboulsi EI, Enger C, Maumenee IH. Glaucoma in the Marfan syndrome. *Transactions of the American Ophthalmological Society* 1992;90:111-117; discussion 118-122.

55. Farias FH, Johnson GS, Taylor JF, et al. An ADAMTS17 splice donor site mutation in dogs with primary lens luxation. *Investigative Ophthalmology & Visual Science* 2010;51:4716-4721.

56. Willett K, Bennett J. Immunology of AAV-Mediated Gene Transfer in the Eye. *Frontiers in Immunology* 2013;4:261.

57. Flotte TR, Carter BJ. Adeno-associated virus vectors for gene therapy. *Gene Therapy* 1995;2:357-362.

58. Buning H, Perabo L, Coutelle O, Quadt-Humme S, Hallek M. Recent developments in adeno-associated virus vector technology. *The Journal of Gene Medicine* 2008;10:717-733.

59. Schultz BR, Chamberlain JS. Recombinant adeno-associated virus transduction and integration. *Molecular Therapy: The Journal of the American Society of Gene Therapy* 2008;16:1189-1199.

60. Muzyczka N. Use of adeno-associated virus as a general transduction vector for mammalian cells. *Current Topics in Microbiology and Immunology* 1992;158:97-129.

61. McLaughlin SK, Collis P, Hermonat PL, Muzyczka N. Adeno-associated virus general transduction vectors: analysis of proviral structures. *Journal of Virology* 1988;62:1963-1973.

62. Petersen-Jones SM. Viral vectors for targeting the canine retina: a review. *Veterinary Ophthalmology* 2012;15 Suppl 2:29-34.

63. Ferrari FK, Samulski T, Shenk T, Samulski RJ. Second-strand synthesis is a rate-limiting step for efficient transduction by recombinant adeno-associated virus vectors. *Journal of Virology* 1996;70:3227-3234.

64. Petersen-Jones SM, Bartoe JT, Fischer AJ, et al. AAV retinal transduction in a large animal model species: comparison of a self-complementary AAV2/5 with a single-stranded AAV2/5 vector. *Molecular Vision* 2009;15:1835-1842.

65. Zhong L, Zhao W, Wu J, et al. A dual role of EGFR protein tyrosine kinase signaling in ubiquitination of AAV2 capsids and viral second-strand DNA synthesis. *Molecular Therapy: The Journal of the American Society of Gene Therapy* 2007;15:1323-1330.

66. Gaasterland D, Kupfer C. Experimental glaucoma in the rhesus monkey. *Investigative Ophthalmology* 1974;13:455-457.

67. Weber AJ, Zelenak D. Experimental glaucoma in the primate induced by latex microspheres. *Journal of Neuroscience Methods* 2001;111:39-48.

68. Teixeira LB, Buhr KA, Bowie O, et al. Quantifying optic nerve axons in a cat glaucoma model by a semi-automated targeted counting method. *Molecular Vision* 2014;20:376-385.

69. Gerometta R, Podos SM, Danias J, Candia OA. Steroid-induced ocular hypertension in normal sheep. *Investigative Ophthalmology & Visual Science* 2009;50:669-673.

70. Gerometta R, Podos SM, Candia OA, et al. Steroid-induced ocular hypertension in normal cattle. *Archives of Ophthalmology* 2004;122:1492-1497.

71. Zhou Y, Grinchuk O, Tomarev SI. Transgenic mice expressing the Tyr437His mutant of human myocilin protein develop glaucoma. *Investigative Ophthalmology & Visual Science* 2008;49:1932-1939.

72. Chi ZL, Akahori M, Obazawa M, et al. Overexpression of optineurin E50K disrupts Rab8 interaction and leads to a progressive retinal degeneration in mice. *Human Molecular Genetics* 2010;19:2606-2615.

73. Aihara M, Lindsey JD, Weinreb RN. Ocular hypertension in mice with a targeted type I collagen mutation. *Investigative Ophthalmology & Visual Science* 2003;44:1581-1585.

74. Filippopoulos T, Danias J, Chen B, Podos SM, Mittag TW. Topographic and morphologic analyses of retinal ganglion cell loss in old DBA/2NNia mice. *Investigative Ophthalmology & Visual Science* 2006;47:1968-1974.

75. Ticho U, Lahav M, Berkowitz S, Yoffe P. Ocular changes in rabbits with corticosteroid-induced ocular hypertension. *The British Journal of Ophthalmology* 1979;63:646-650.

76. Veth KN, Willer JR, Collery RF, et al. Mutations in zebrafish lrp2 result in adult-onset ocular pathogenesis that models myopia and other risk factors for glaucoma. *PLoS Genetics* 2011;7:e1001310.

CHAPTER 3 – MATERIALS AND METHODS

Study Design

This research project encompasses controlled non-randomized experiments. Four cohorts of dogs were established: three evaluated the efficiency of recombinant AAV, and one examined drug effects on IOP. In all AAV studies (cohorts 1, 2, and 3), intracameral injection of the vector was administered to the right eye. The left eye did not receive any type of injection and served as the control. In cohort 4, both eyes were tested.

Cohort 1 contained *wt* beagle dogs (n=6) between the ages of 4-8 months with baseline IOPs between 10-20 mmHg. The aim was to target *wt* TM cells with AAV-capsid mutant vectors containing GFP cDNA. Cohort 2 consisted of *ADAMTS10*-mutant beagle-derived mongrel dogs (n=4) ~1 year of age with IOPs < 40 mmHg. This experiment investigated the efficiency of viral vectors in transducing mutant TM cells. In both cohorts, the primary outcome measure was GFP expression in tissue samples assessed by IHC. Potential adverse effects, such as immune reactions, were monitored through ophthalmic examinations and variations in IOP.

Cohort 3 comprised of both pre-glaucomatous (n=7) and glaucomatous (n=3) *ADAMTS10*-mutant, beagle-derived mongrel dogs. Pre-glaucomatous dogs were < 2 years of age with IOP < 40 mmHg. Glaucomatous dogs were of any age and had sustained elevated IOP (> 40 mmHg) in one or both eyes. The goal was to target human *wt ADAMTS10* cDNA to TM cells in mutant beagles, and provide evidence of gene augmentation by lowering and/or preventing ocular hypertension. The main output measure for this cohort was weekly diurnal IOPs collected for 19 weeks.

Cohort 4 was added later to study with the intention of characterizing the subacute increase in pressure observed during the preliminary assessment of the post-injection IOP data. Previous studies reported that prolonged use of topical dexamethasone lead to transient ocular hypertension in glaucomatous beagles.[1] All AAV-treated dogs in our study received a 4-week post-injection treatment with glucocorticoids in order to prevent potential vector-induced uveitis. Since the drugs may mask the therapeutic effect initiated by gene replacement therapy, we created a side-project to monitor the effect of standard glucocorticoid medication on IOP in eyes not treated with AAV. The experiment included *ADAMTS10*-mutant (n=3) and carrier (n=1) beagle-derived mongrel dogs between the ages of 4-8 months with baseline IOP between 10-20 mmHg. The key outcome measure was weekly diurnal pressures analyzed for 12 weeks.

Animals

For cohort 1, normal beagle dogs (n=6 male dogs; median age at injection 4.6 months, range 4.5 – 4.8 months) were obtained from a commercial supplier (Marshal Bioresources, North Rose, NY, USA; Table 3.1). For cohorts 2, 3, and 4, *ADAMTS10*-mutant dogs (n=17; 10 males and 7 females; median age at injection 18.2 months, range 7.6 -63.8 months) and one *ADAMTS10*-mutant carrier (female; age at injection 7.6 months) were part of a canine POAG colony at MSU of beagle-derived mongrel dogs carrying the G661R missense mutation (Table 3.1). The *ADAMTS10* genotype was determined by PCR, gel electrophoresis, and Sanger sequencing either at the MSU Research Technology Support Facility or at a commercial testing laboratory (OptiGen® LLC, Ithaca, NY, USA). The animals were housed at the Vivarium of the MSU College of Veterinary Medicine under a 12 hour light:dark cycle.

Table 3.1 Summary of the cohorts.

	AAV	Treated eye	Vector concentration (vg/ml) and volume (µl)	Dog ID/gender	Genotype	Age at injection (months)	Measurement of pre-injection IOP (weeks)	Measurement of post-injection IOP (weeks)	IHC time points (week)
Cohort 1	*AAV2(Y444F)-GFP*	R	2×10^{12} vg/ml (50 µl)	5555/m	*wt*	4.8	4	6	8
			2×10^{10} vg/ml (50 µl)	70176/m	*wt*	4.5	4	6	11
	AAV2(Triple Y-F)-GFP		2×10^{12} vg/ml (50 µl)	1270/m	*wt*	4.6	4	6	8
	AAV2(Triple Y-F + T-V)-GFP		2×10^{12} vg/ml (50 µl)	9615/m	*wt*	4.5	4	6	8
	AAV2(Triple Y-F)-GFP	R	2×10^{10} vg/ml (50 µl)	1512/m	*wt*	4.6	4	6	20
	AAV2(Y444F)-GFP	L[a]	2×10^{11} vg/ml (50 µl)				12	6	7
	AAV2(Triple Y-F + T-V)-GFP	R	2×10^{10} vg/ml (50 µl)	5580/m	*wt*	4.8	4	6	20
	AAV2(Y444F)-GFP	L[a]	2×10^{12} vg/ml (50 µl)				12	6	7
Cohort 2	*AAV2(Y444F)-GFP*	R	2×10^{12} vg/ml (50 µl)	3277/f	*ADAMTS10*- mutant	13.7	10	10	14
				5877/f	*ADAMTS10*- mutant	13.7	10	6	7
			2×10^{11} vg/ml (50 µl)	7930/m	*ADAMTS10*- mutant	13.7	10	10	14
				6366/m	*ADAMTS10*- mutant	13.7	2	6	7
Cohort 3	*AAV2(Y444F)-hADAMTS10*	R	2×10^{12} vg/ml (50 µl)	97930/f	*ADAMTS10*- mutant	18.3	13	19	
Pre-				6623/m	*ADAMTS10*- mutant	18.2	13	19	
glaucomatous				7869/m	*ADAMTS10*- mutant	18.3	13	19	
				1259/m	*ADAMTS10*- mutant	21.6	13	19	
				1331/m	*ADAMTS10*- mutant	21.4	13	19	
				7457/f	*ADAMTS10*- mutant	21.6	13	19	
				6941/m	*ADAMTS10*- mutant	21.6	1	8	
Glaucomatous	*AAV2(Y444F)-hADAMTS10*	R	2×10^{12} vg/ml (50 µl)	10166/f[b]	*ADAMTS10*- mutant	21.4	13	19	
				G19/m[b]	*ADAMTS10*- mutant	57.8	13	18	
				G3/m	*ADAMTS10*- mutant	63.8	13	1	
Cohort 4		R/L		1971/f	*ADAMTS10*- carrier	7.6	2	12	
Steroid				90830/f	*ADAMTS10*- mutant	7.6	2	12	
Response Test				1522/f	*ADAMTS10*- mutant	7.6	2	12	
				1447/m	*ADAMTS10*- mutant	7.6	2	12	

Adeno-associated virus (AAV): AAV serotype 2 (AAV2), capsid mutant Y-F (Y444F, Y500F, Y730F), T-V (T491V), green fluorescent protein (GFP), *wild type* human *ADAMTS10* (*hADAMTS10*); treated eye: right (R), left (L), both (R/L); vector concentration: vector genome per milliliter (vg/mL); gender: male (m), female (f); genotype: *wild type* (*wt*), G661A variant in *ADAMTS10* (*ADAMTS10*-mutant); intraocular pressure (IOP); immunohistochemistry (IHC); [a]Readministration of AAV; [b]Included in 'challenge' trial.

All studies were conducted in compliance with the Association for Research in Vision and Ophthalmology statement for Use of Animals in Ophthalmic and Vision Research and approved by the MSU Institutional Animal Care and Use Committee and Institutional Biosafety Committee.

AAV constructs

The production of the non-self-complementary recombinant AAV serotype 2 vectors was accomplished by the Hauswirth lab at the University of Florida, Gainesville, FL, USA. The purification and concentration methods have been previously described.[2, 3] Succinctly, site-directed mutagenesis was performed on AAV helper plasmids containing AAV2 "Cap" to incorporate mutations to surface exposed tyrosine and/or threonine residues of the capsids. The vectors were generated by plasmid co-transfection in HEK293T cells. The nuclear and cytoplasmic fractions was further purified and concentrated by iodixanol (Sigma-Aldrich, St. Louis, MO, USA) gradient centrifugation and ion exchange column chromatography (HiTrap Sp Hp 5 mL, GE Healthcare Bio-Sciences, Piscataway, NJ, USA). The vector titer and purity was established by real-time PCR and silver-stained sodium dodecyl sulfate-polyacrylamide gel electrophoresis, respectively. Final aliquots were resuspended in BSS (BSS Alcon Laboratories, Forth Worth, TX, USA) containing 0.014% Tween 20.

The vectors were driven by a ubiquitous smCBA (Figure 3.1). Three types of mutant vectors were chosen for the study: single (Y444F), triple (Y444,500,730F), and quadruple (Y444,500,730F + T491V) (Table 3.1). The vectors either carried GFP (cohort 1 and 2) or *wt* human *ADAMTS10* cDNA (cohort 3).

Figure 3.1 Map of vector plasmids. Ubiquitous chicken beta-actin promoter (smCBA) was used in AAV vectors carrying either (A) GFP or (B) *hADAMTS10* cDNA.

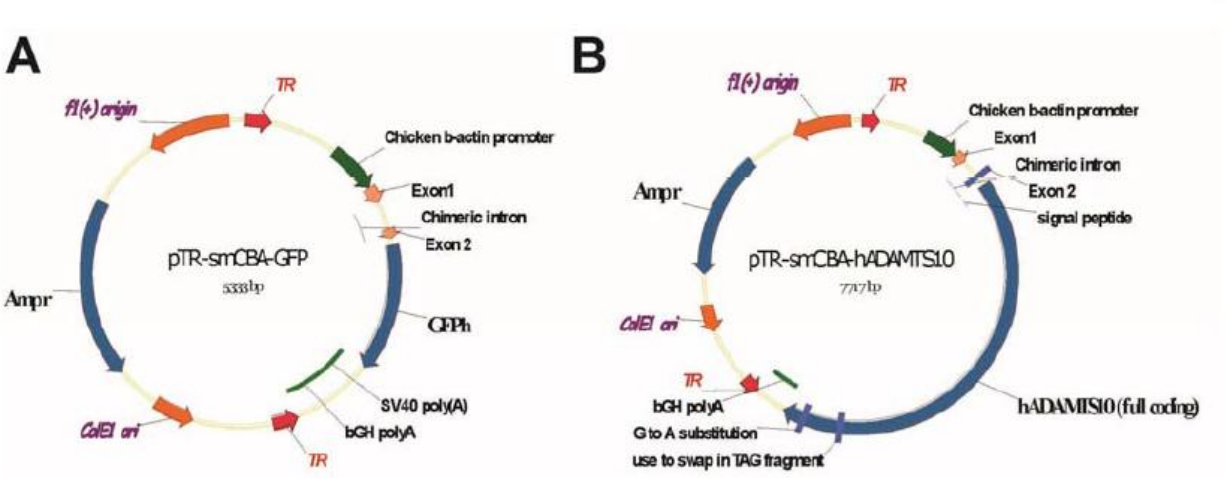

The *hADAMTS10* coding sequence (~3.3 kb) was synthesized according to Genbank accession number NM_030957 with the addition of consensus 'kozak' sequence and a silent G to A change in nucleotide 3150. The full mRNA (~4.3 kb) includes 5' and 3 un-translated regions, which were dropped in order to fit the coding sequence within an AAV vector. The silent substitution removed an internal Not I restriction enzyme site. The synthetic cDNA was subsequently cloned into the AAV vector plasmid containing the smCBA promoter following Not I/Sal I digest.

Intracameral injections

The AAV administration procedure remained relatively consistent for each cohort: the right eye received the vector, the left eye operated as the control, and both eyes received pre- and post-operative steroids, NSAIDs, and antibiotics as prophylaxis against sterile immune reactions post-surgery, bacterial infections, and inflammatory responses against the viral vector and/or transgene. This format eliminated any additional confounding variables that may affect IOP. Pre-operatively the dogs received prednisone 20 mg (Roxane Laboratories, Inc., Columbus, OH, USA; 1 mg/kg oral), amoxicillin/clavulanic acid (Clavamox, Zoetis, Florham Park, NJ, USA; 12.5 mg/kg oral), in addition to three drops, 30 minutes apart, of flurbiprofen sodium 0.03% (Bausch & Lomb Inc., Tampa, FL, USA) and one drop of prednisone acetate 1% (Pacific Pharma, Irvine, CA, USA) ophthalmic solutions. Post-operatively, both eyes received a subconjunctival injection of triamcinolone acetonide injectable suspension 4 mg (Kenalog®-40, Bristol-Myers Squibb Company, Italy), followed by atropine sulfate 1% (Bausch & Lomb Inc., Tampa, FL, USA) and neomycin and polymyxin B sulfates and dexamethasone (Bausch & Lomb Inc., Tampa, FL, USA) ophthalmic ointments. The dogs were given tapering doses of prednisone (1 mg/kg oral; twice daily for 7 days, once daily for 8 days, and every other day for 6 days), and amoxicillin/clavulanic acid (12.5 mg/kg oral; twice daily for 4 days). Ophthalmic treatment for

both eyes included neomycin and polymyxin B sulfates and dexamethasone (eye ointment; twice daily for 21 days, and once daily for 5 days), and atropine (eye ointment; twice daily for 4 days, and once daily for 5 days). Note that atropine was excluded from the mutant cohorts because its long-acting mydriatic properties can further increase in IOP in these dogs.[4] The glaucomatous dogs were also maintained on IOP-reducing medications; dorzolamide hydrochloride-timolol maleate (Bausch & Lomb Inc., Tampa, FL, USA) and/or latanoprost 0.005% (Greenstone LLC., Peapack, NJ, USA) ophthalmic solutions.

The dogs were premedicated with acepromazine maleate injection (Butler Schein Animal Health, Dublin, OH, USA; 0.2 mg/kg IM), and induced and maintained under anesthesia with intravenous propofol (PropoFlo™28, Abbott Laboratories, North Chicago, IL, USA; 4mg/kg). They were positioned in sternal recumbency, and one ocular surface was anesthetized with proparacaine hydrochloride 0.5% ophthalmic solution (Bausch & Lomb Inc., Tampa, FL, USA) and aseptically prepped with povidone iodine 10% swabsticks (Dynarex Corporation, Orangeburg, NY, USA). Vector solutions were diluted with sterile balanced salt solution (BSS, Alcon Laboratories, Inc., Forth Worth, TX, USA) and drawn into 1cc tuberculin (26 gauge x ½ needle) or insulin syringes (30 gauge x 1/2 inch needle). The superior-temporal limbus of the eye was visualized by a binocular loupe (EyeMag Pro, Carl Zeiss Inc., Oberkochen, Germany) with illumination, and the needle was introduced into the anterior chamber at an oblique angle, parallel to the iris surface for several millimeters with the tip angled (Figure 3.2). Fluid entry of the AAV preparation (50 μL) was carefully observed. The needle was left in place for 1-10 minutes, before being withdrawn in order to minimize reflux/escape of vector solution. The injection site was held off for 2 minutes, and fluid leakage was assessed.

Figure 3.2 Example of an intracameral injection. The animal was under general anesthesia and the ocular surface was anesthetized with topical proparacaine 0.5% ophthalmic solution. Toothed Castroviejo suture forceps were used to secure and immobilize the eye. A wire lid speculum maintained palpebral fissure open. The needle was introduced into the anterior chamber at the superior-temporal limbus.

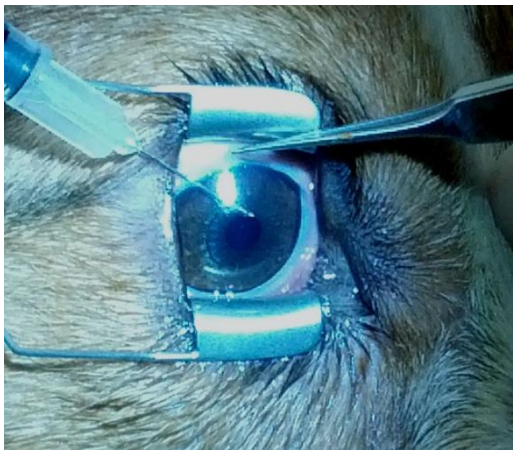

Cohort 1 received different AAV-capsid mutant vectors carrying GFP at either 2 x 10^{10} vg/mL or 2 x 10^{12} vg/mL (Table 3.1). Once it became clear that AAV2(Y444F) was the best capsid mutant to target the canine TM, two dogs from same study were re-injected in the contralateral eye three months later (Table 3.1). The objective was to confirm the reporter gene expression results, evaluate any dosing effect, and assess potential inflammatory reactions from vector re-administration. *AAV2(Y444F)-GFP* was administered to cohort 2 at either 2 x 10^{11} vg/mL or 2 x 10^{12} vg/mL (Table 3.1). Cohort 3 received *AAV2(Y444F)-hADAMTS10* at 2 x 10^{12} vg/mL (Table 3.1).

Tonometry

Baseline (pre-injection) and follow-up (post-injection) IOPs were assessed in all groups (Table 3.1). Diurnal IOPs (8AM, 11AM, 2PM) were collected once a week by one examiner (AO) with a tonometer. Pressures were assessed throughout the day in order to address the circadian variations in IOP present in dogs; pressures are higher in the morning compared to the early evening.[5, 6] The first cohort was initially measured with Tono-Pen VET™ Veterinary Tonometer applanation (Reichert Inc., Depew, NY, USA), but was later transitioned to Tonovet™ rebound (Icare Finland, Vantaa, Finland). Applanation and rebound tonometers both provide consistent IOP measurements in normotensive subjects.[7] However, the rebound tonometer has been proven to be more accurate in ocular hypertensive patients and does not require topical anesthetics.[8] As a result, cohorts 2, 3, and 4 were only assessed with the Tonovet™ , and differences between tonometers will not be further discussed.

Because any therapeutic effect of the AAV vector was likely masked by the routine use of IOP-lowering medications, a ‘challenge’ trial was performed in two glaucomatous dogs (Table

3.1). The purpose was to observe if the AAV treatment alone was sufficient to keep the IOP controlled. The medications were usually given twice daily (morning and late afternoon). At 2 and 4 months post-injection, the morning regimen was discontinued and IOPs were evaluated throughout the day.

Steroid response test

To evaluate the confounding effects of steroids, *ADAMTS10*-mutant dogs (n=3) and an *ADAMTS10*-carrier (n=1) were included in a steroid response test (Table 3.1). The dogs were littermates and of the same age. Both eyes received neomycin and polymyxin B sulfates and dexamethasone ophthalmic ointment twice a day for 4 weeks. Diurnal IOPs (8AM, 11AM, 2PM) were measured once a week for 2 weeks prior, 4 weeks during, and 12 weeks after the steroid treatment.

Ophthalmic examination

Regular ophthalmic examinations were performed pre-injection, immediately post-injection for 2 days daily, twice per week for 2 weeks, and then weekly to bi-weekly until the end of each study. Anterior segments were examined for clarity and cells with diffuse and focal illumination using portable hand-held slit-lamp biomicroscopes (Kowa SL14; Kowa Company, Tokyo, Japan). Fundic examinations were performed with portable binocular indirect ophthalmoscopes (Keeler All Pupil II; Keeler Instruments, Broomall, PA, USA) and condensing lens (Pan Retinal 2.2D; Volk Optical, Mentor, OH, USA). The ICA angle width was evaluated with gonioscopy: the ocular surface was anesthetized with proparacaine hydrochloride 0.5% ophthalmic solution and the ICA was imaged with RetCam II (Clarity Medical Systems, Pleasanton, CA, USA).

RetCam II and cSLO were both used to evaluate *in vivo* GFP expression in the ICA. With cSLO, the dogs were placed under anesthesia, and one drop of proparacaine hydrochloride 0.5% provided ocular surface anesthesia as a gonioscopic lens (G-4 Goniolaser, Volk, Mentor, OH, USA) was placed on the corneal surface. The ICA was imaged under Infrared Reflectance and BluePeak™ blue laser autofluorescence with a 55° lens (Spectralis®, Heidelberg Engineering, Heidelberg, Germany).

Tissue processing/sectioning

GFP expression was analyzed at multiple time points for cohort 1 and 2 (Table 3.1). The subjects were euthanized by barbiturate overdose (Fatal Plus, Vortech Pharmaceuticals, Dearborn, MI, USA). The eyes were enucleated and a 2-mm slit was made along the pars plana of the globe. Approximately 0.5 mL of 4% paraformaldehyde in PBS was injected intravitreally through the slit and the globe was then placed in 25 mL of the same solution and stored at 4°C. Three hours later, the anterior segment was then separated from the posterior portion of the eye and the vitreous was discarded. The two halves were subsequently placed in 2% paraformaldehyde and stored at 4°C for 24 hours. The tissues were then transferred to 15% and 30% sucrose in PBS at 4°C for 24 hours each.

The anterior segment including lens, was cut into 4 even quadrants, superior-nasal (SN), inferior-nasal (IN), inferior-temporal (IT), and superior-temporal (ST) (Figure 3.3), and embedded in optical cutting temperature medium (Tissue-Tek OCT, Sakura Finetek USA Inc., Torrence, CA, USA), and stored at -80°C. Prior to sectioning, the eyes were kept at -20°C for ~20 minutes.

Figure 3.3 Four quadrants of the anterior segment. The anterior segment of the right and left eye was divided into four quadrants: superior-nasal (SN), inferior-nasal (IN), inferior-temporal (IT), and superior-temporal (ST). In this diagram, the cornea is facing down.

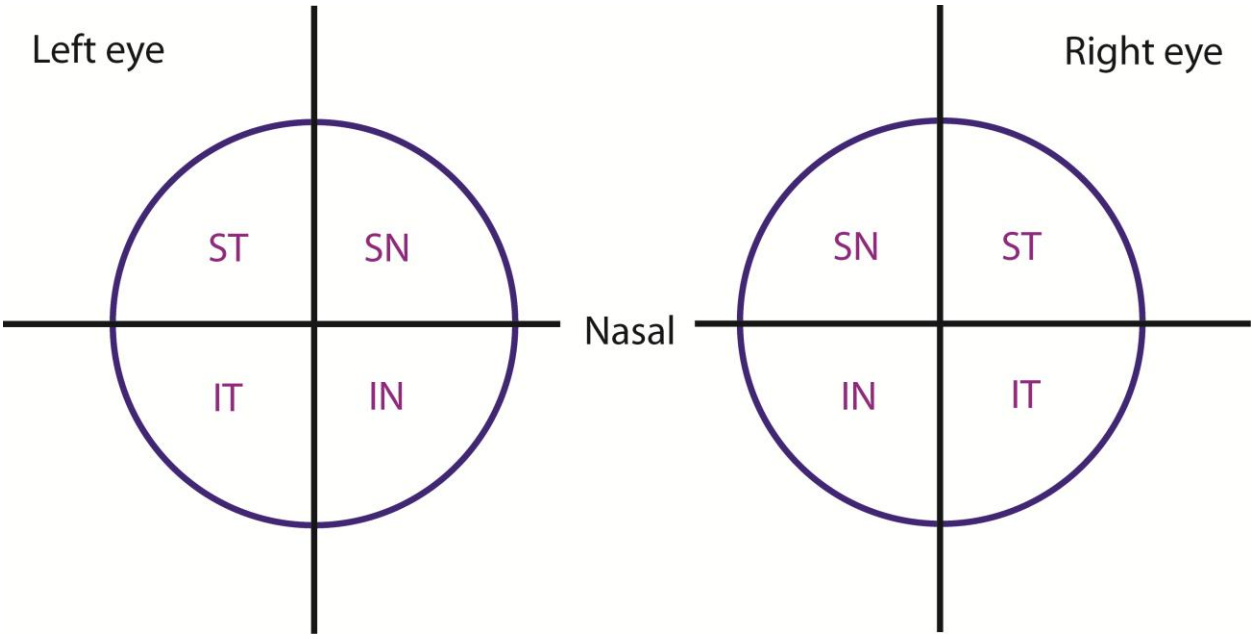

Fourteen micrometer transverse anterior segment cyrosections were collected using a cryomicrotome (Leica CM3050-S, Leica Microsystems, Buffalo Grove, IL, USA) onto charged microscope glass slides (Adhesion Superfrost Plus, Brain Research Laboratories, Newton, MA, USA). The slides were dried for 20 minutes and stored in 4°C.

Immunohistochemistry and image analysis

The same reagents and basic protocol were used for all tissue samples. The slides were warmed to room temperature, rehydrated for 35 minutes in PBS containing detergent 0.1% Triton X-100, and then blocked in 5% serum (Normal Goat Serum, 1:20, Jackson ImmunoResearch Laboratories, Inc., West Grove, PA, USA). The slides were washed with PBS for 10 minutes. The primary anti-GFP, rabbit polyclonal antibody (AlexaFluor® 594, 1:1000, Life Technologies, Eugene, OR, USA) was incubated overnight at 4°C. After the slides were washed for 25 minutes in PBS, they were mounted using antifade reagent with DAPI (ProLong® Gold, Life Technologies, Eugene, OR, USA) and glass coverslips (Electron Microscopy Sciences, Hatfield, MO, USA). All slides were stored at 4°C in the dark. Since native GFP was relatively weak, enhanced GFP with immunolabeling was analyzed. Semi-quantitative analysis of enhanced GFP was completed with fluorescent microscopy (Eclipse 80i Fluorescent Microscope, Nikon Instruments Inc., Melville, NY, USA). Each quadrant was graded by a non-blinded observer (AO) on a scale of 1-5 (1=absent; 2 = weak; 3 = moderate; 4 = strong; 5 = very strong), and reported values were averaged. Approximately 8 sections per quadrant were analyzed for the *wt* group and 16 sections per quadrant were analyzed for the mutant group. The slides were then imaged with the fluorescent or confocal microscopy (FV1000 Laser Scanning Confocal Microscope, Olympus America Inc., Center Valley, PA, USA) at x 10, x 20, x 40, and x 120 magnification.

Statistical analysis

In cohort 3, the primary outcome measure was IOP. A power calculation using a two-sided paired t-test revealed that a sample size of seven *ADAMTS10*-mutant dogs would provide 90% power to detect a 6-mmHg decrease in IOP of the treated eye compared to the control eye with a significance level (alpha) of 0.05, assuming the standard deviation of the measured IOPs is 4 mmHg. To adjust the correlation in IOP from two eyes measured at multiple visits, a generalized linear model using generalized estimating equation (GEE) Wald test was performed. IOP was a primary outcome measure for cohort 4 and a secondary outcome measure for cohorts 1 and 2. Even though the sample sizes were small, a generalized linear model using GEE Wald test was used to estimate the average IOP response.

Selected IOP data points were excluded or abbreviated (Table 4.2). Exclusion criteria were correspondingly established to decrease variability and increase accuracy of reported data. Subjects that were added later to their respective cohorts had abbreviated pre-injection pressures, and data was excluded from those that were euthanized prior to the end of the study. Since IOP-lowering medications are a confounding variable, pressure records from treated eyes were excluded from the statistical analysis. Specific omissions are further explained in the results section.

REFERENCES

REFERENCES

1. Gelatt KN, Mackay EO. The ocular hypertensive effects of topical 0.1% dexamethasone in beagles with inherited glaucoma. *Journal of Ocular Pharmacology and Therapeutics: The Official Journal of the Association for Ocular Pharmacology and Therapeutics* 1998;14:57-66.

2. Zolotukhin S, Potter M, Zolotukhin I, et al. Production and purification of serotype 1, 2, and 5 recombinant adeno-associated viral vectors. *Methods* 2002;28:158-167.

3. Jacobson SG, Acland GM, Aguirre GD, et al. Safety of recombinant adeno-associated virus type 2-RPE65 vector delivered by ocular subretinal injection. *Molecular Therapy: The Journal of the American Society of Gene Therapy* 2006;13:1074-1084.

4. Grozdanic SD, Kecova H, Harper MM, Nilaweera W, Kuehn MH, Kardon RH. Functional and structural changes in a canine model of hereditary primary angle-closure glaucoma. *Investigative Ophthalmology & Visual Science* 2010;51:255-263.

5. Giannetto C, Piccione G, Giudice E. Daytime profile of the intraocular pressure and tear production in normal dog. *Veterinary Ophthalmology* 2009;12:302-305.

6. Gelatt KN, Gum GG, Barrie KP, Williams LH. Diurnal variations in intraocular pressure in normotensive and glaucomatous Beagles. *Glaucoma* 1981;3:21-24.

7. Leiva M, Naranjo C, Pena MT. Comparison of the rebound tonometer (ICare) to the applanation tonometer (Tonopen XL) in normotensive dogs. *Veterinary Ophthalmology* 2006;9:17-21.

8. McLellan GJ, Kemmerling JP, Kiland JA. Validation of the TonoVet(R) rebound tonometer in normal and glaucomatous cats. *Veterinary Ophthalmology* 2013;16:111-118.

CHAPTER 4 - RESULTS

AAV2(Y444F) targets GFP expression to the canine wt ICA

Initial intracameral injection of the single stranded AAV2(Y444F) vector successfully targeted GFP expression to *wt* cells located along the aqueous humor outflow pathways (Figure 4.1A). Reporter gene expression was present at both concentrations (2×10^{10} and 2×10^{12} vg/mL; 50 µL); though a modest dosing effect without immunolabeling was observed over the two log units on subjective assessment. The overall expression was relatively weak with many presumed cells remaining GFP negative, but native GFP fluorescence was enhanced with immunolabeling and positive cells were still observed at 8 and 11 weeks post-injection. *In vivo* GFP fluorescence was not observed in the ICA by gonioscopy.

Consistent with previous descriptions of TM morphology,[1] the cells appeared broad to spindle shaped with long cytoplasmic processes (Figure 4.1B). The molecular characterization of these cells is planned for the future; it requires a combination of antibodies for IHC (Table 5.1). GFP expression was detected in all four quadrants with no obvious difference, demonstrating successful widespread delivery of the vector to the ICA (Table 4.1). Despite stronger presumed transduction efficiency in murine retinal cells and hepatocytes compared to AAV2(Y444F), [2-4] positive cells were absent with AAV2(Triple T-F) and AAV2(Y-F + T-V) capsid based mutant vectors (Figure 4.1C).

Even with a ubiquitous smCBA promoter, GFP expression was rather specific with almost exclusive fluorescence along the aqueous humor outflow pathways. Nevertheless, transduction of AAV2(Y444F) was not limited to cells within the ICA as uniform expression was observed on the anterior border layer of the iris (Figure 4.1A; *arrow*). Transduced cells of

the anterior border of the iris were spindle-shaped, and at times displayed stronger fluorescence than the cells in the ICA (Figure 4.1D).

AAV2(Y444F) targets GFP expression to the canine ADAMTS10-mutant ICA.

Based on the results with AAV2(Y444F), mutant eyes were injected with *AAV2(Y444F)-hADAMTS10* at the highest dose (2×10^{12} vg/mL; 50 μL). Consistent with the findings from the first cohort, GFP transduction was found along the aqueous humor outflow pathways (Figure 4.2A), observed at both post-injection time points (7 and 14 weeks), and detected in each ICA quadrant (Table 4.1; Figure 4.2B). *In vivo* GFP fluorescence in the ICA was also not detected by gonioscopy.

The morphology of the transduced mutant cells was also similar to the *wt* cells and consistent with TM cells (Figure 4.2C). Though, further molecular testing of the cell would be required to confirm this, as fibroblasts can be misidentified as TM cells. Positive spindle-shaped cells (Figure 4.2D) were also noted along the length of the anterior border of the iris (Figure 4.2A, *arrow*). Contrary to the *wt* canines, GFP expression was consistently present along the posterior pigmented epithelial layer of the iris (Figure 4.3). Fluorescence was mainly observed on the pupillary margin.

Therapeutic effect of AAV2(Y444F)-hADAMTS10

A single intracameral injection of *AAV2(Y444F)-hADAMTS10* revealed no observable therapeutic effect on IOP over 19 weeks. Both pre-glaucomatous (n=7) and glaucomatous (n=3) mutant dogs received the vector at the highest dose (2×10^{12} vg/mL; 50 μL). A therapeutic

Figure 4.1 ICA of *wt* dogs. (A) Only *AAV2(Y444F)-GFP* showed positive native GFP expression (*green*). GFP expression was found in the ICA and on the anterior border layer of the iris (*arrow*). GFP fluorescence was enhanced with anti-GFP antibody (*red*). Overlay of images (*yellow*) with DAPI stain. Yellow indicates strongest GFP expression, while red means weaker expression. Un-injected control reveals absence of GFP fluorescence. Calibration bar = 50 µm; (B) Magnification of transduced cells. Calibration bar = 10 µm*;* (C) GFP expression was not detected in the eye injected with *AAV2(Triple T-F)* or *AAV2(Y-F + T-V)*. Calibration bar = 50 µm; (D) Cells of the anterior border layer of the iris express GFP. Calibration bar = 10 µm.

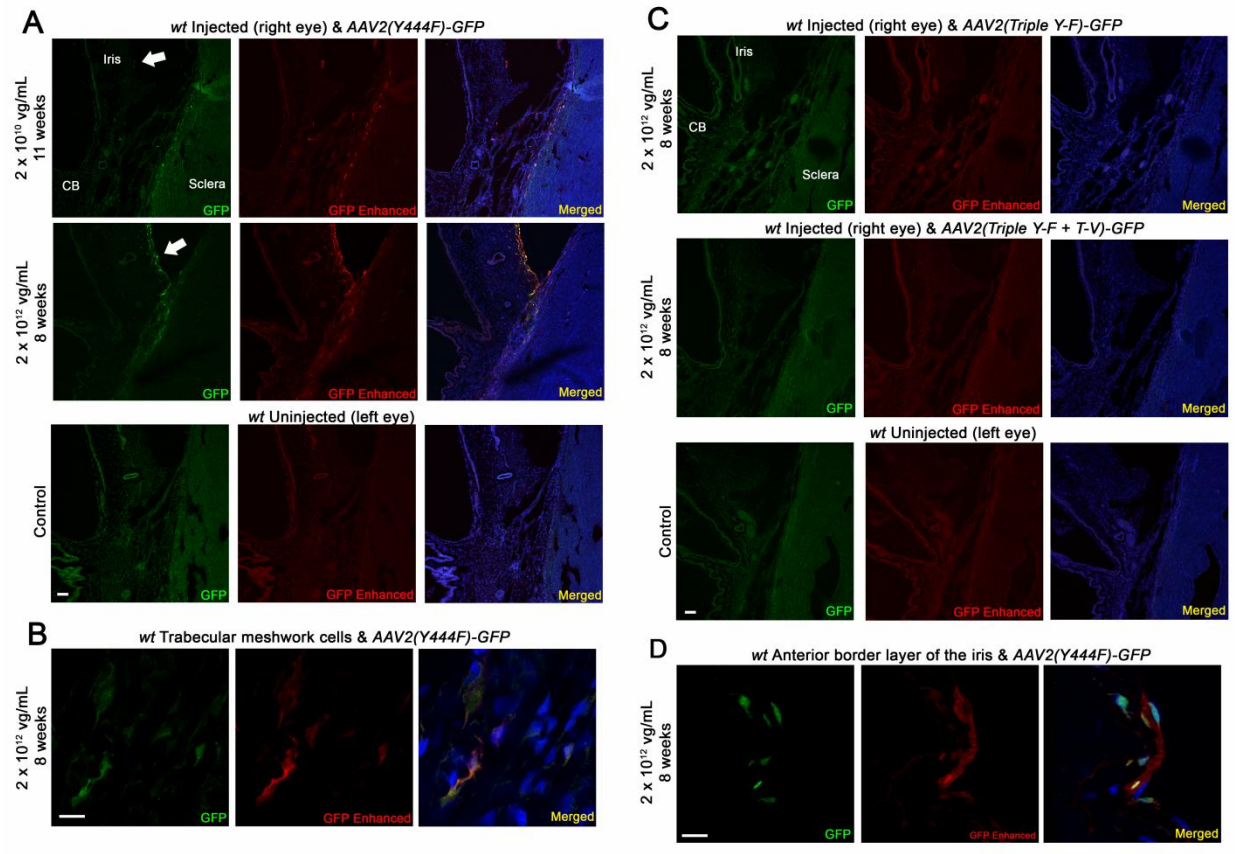

Table 4.1 Semi-quantitative analysis of GFP expression.

	Treated eye	Vector concentration (vg/ml) and volume (µl)	Dog ID/gender	Genotype	AS1	AS2	AS3	AS4
Cohort 1	R	2×10^{12} vg/ml (50 µl)	5555/m	*wt*	5.0	2.0	4.0	3.0
AAV2(Y444F)-GFP	R	2×10^{10} vg/ml (50 µl)	70176/m	*wt*	3.4	2.0	4.0	4.0
	L[a]	2×10^{12} vg/ml (50 µl)	5580/m	*wt*	3.0	3.0	3.0	3.0
	L[a]	2×10^{11} vg/ml (50 µl)	1512/m	*wt*	4.0	3.5	4.0	4.0
Cohort 2	R	2×10^{12} vg/ml (50 µl)	3277/f	*ADAMTS10* -mutant	3.8	4.0	2.3	2.0
AAV2(Y444F)-GFP	R		5877/f	*ADAMTS10*- mutant	4.0	3.0	3.5	4.0
	R	2×10^{11} vg/ml (50 µl)	7930/m	*ADAMTS10*- mutant	2.5	2.8	2.3	4.0
	R		6366/m	*ADAMTS10-mutant*	3.5	3.3	3.7	2.0

Adeno-associated virus (AAV): AAV serotype 2 (AAV2), capsid mutant Y444F, green fluorescent protein (GFP); treated eye: right(R), left (L); vector concentration: vector genome per milliliter (vg/mL); gender: male (m), female (f); genotype: *wild type* (*wt*), G661R variant in *ADAMTS10* (*ADAMTS10*-mutant); Anterior segment (AS): 1=absent, 2 = weak, 3 = moderate, 4 = strong, 5 = very strong; [a]Readministration of AAV.

Figure 4.2 ICA of *ADAMTS10*-mutant dogs. (A) *AAV2(Y444F)-GFP* showed positive GFP expression (*green*) in the ICA and anterior border layer of the iris (*arrow*). GFP fluorescence was enhanced with indirect immunofluorescence (*red*). Overlay of native and enhanced GFP images (*yellow*) with DAPI stain. Presence of yellow indicates strongest GFP expression, while red means weaker expression. Un-injected control reveals absence of GFP positive cells. Calibration bar = 50 µm; (B) GFP fluorescence was detected in all four quadrants of the ICA. Calibration bar = 50 µm; (C) Transduced cells express GFP. Calibration bar = 10 µm; (D) Magnification of the anterior border layer of the iris. Calibration bar = 10 µm.

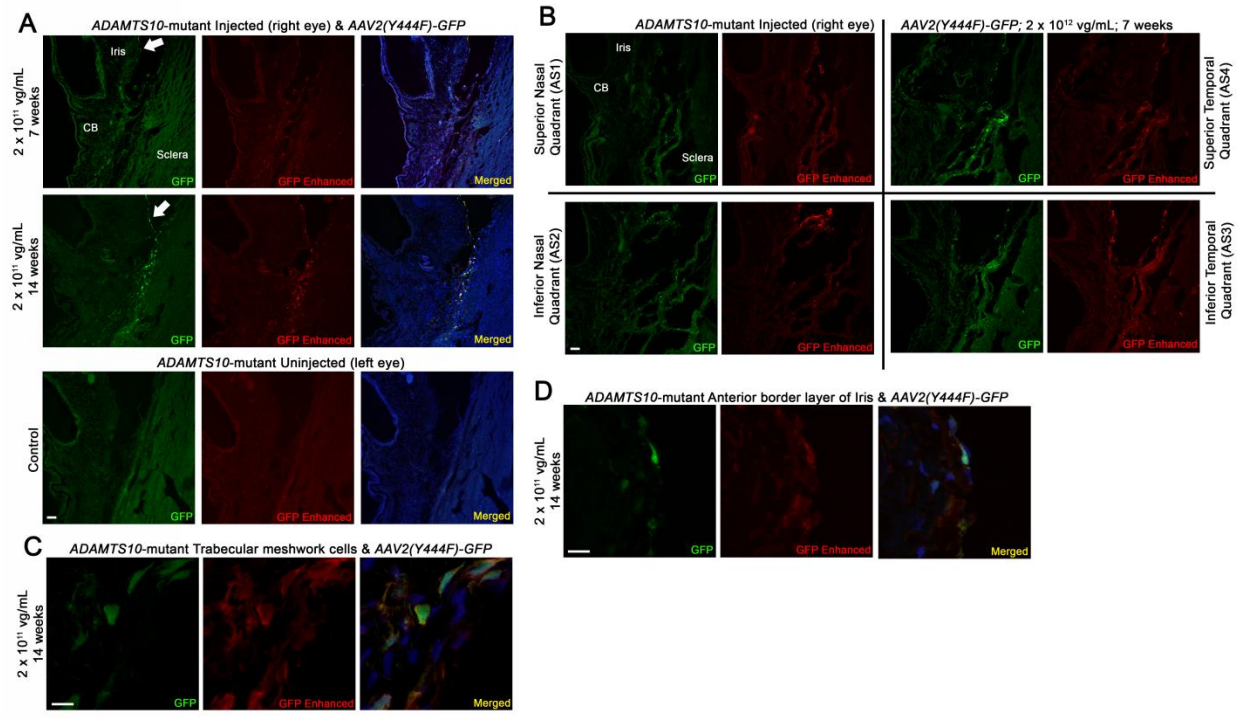

Figure 4.3 Posterior pupillary margin of iris of *ADAMTS10*-mutant dogs. Positive native GFP expression (*green*) at pupillary margin (*arrow*); Expression was enhanced with anti-GFP antibody (*red*). Calibration = 100 µm.

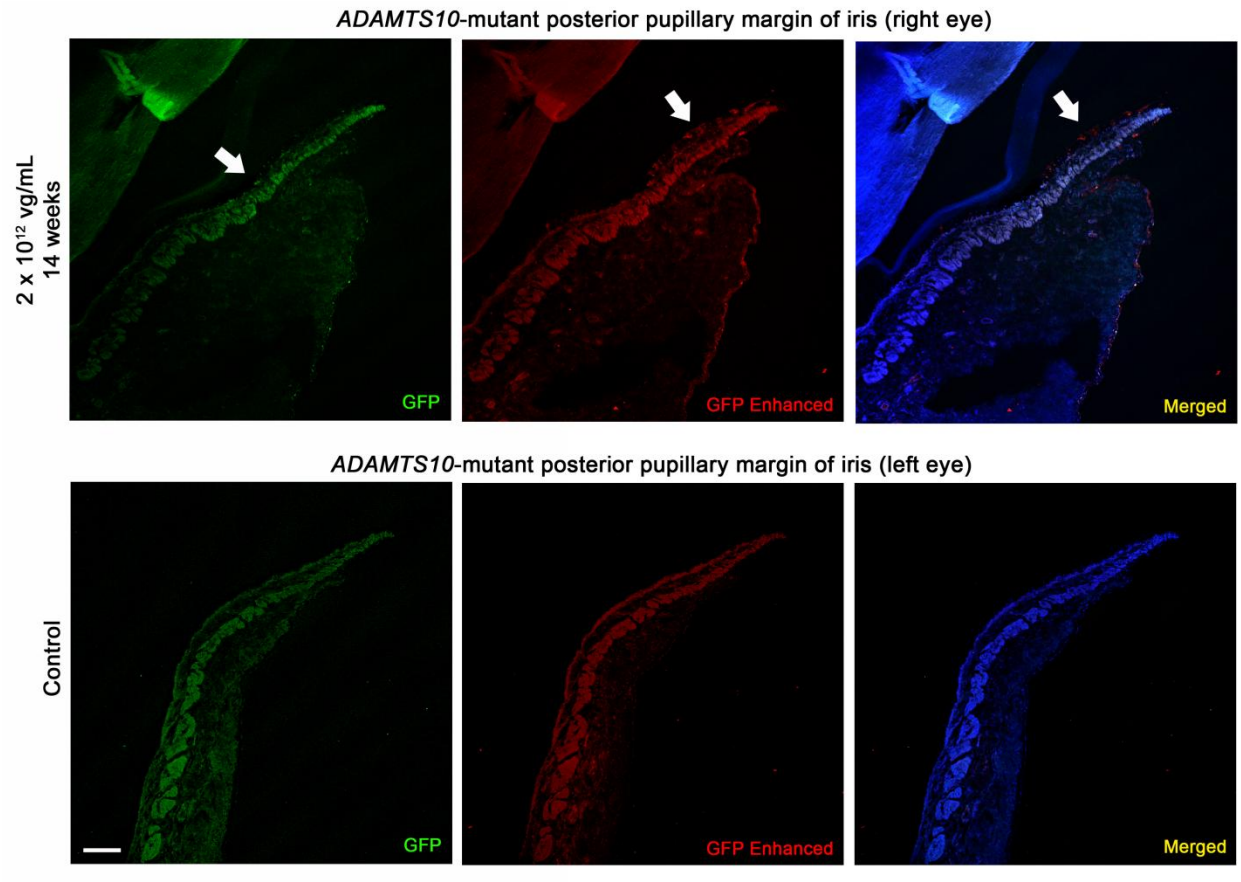

effect would indicate an absence of progressive ocular hypertension and pressure spikes in the injected eye, while a gradual increase in pressure is observed in the control.

IOP data (mean ± standard error) collected with a rebound tonometer revealed a steady bilateral increase in pressures over time in the pre-glaucomatous group (Figure 4.4). IOP averages between the injected (25.0 ± 1.03 mmHg) and control (24.4 ± 1.15 mmHg) eyes also showed no significant difference ($p = 0.56$) with a generalized linear model using GEE Wald test (Table 4.3). Furthermore one dog developed ocular hypertension 11 weeks post-injection (Table 4.2).

In the glaucomatous eyes, we expected that the AAV treatment alone could keep the IOP controlled. However in the two dogs that were part of the 'challenge' trial (Table 4.2), pressures were above 40 mmHg within ~19 hours from the last instillation of medications (data not shown). The glaucomatous groups' IOPs were excluded from further statistical analysis because they had been treated with IOP-lowering medications. Additionally, two dogs were euthanized before the end of the study due to systemic illnesses unrelated to our vector or medical treatments.

Steroid responsiveness of ADAMTS10-mutants and carrier

From preliminary data from cohorts 1 and 2, we assumed that IOP increased with oral and topical glucocorticoid treatment (Figure 4.5; *arrows*). Subsequent statistical analysis (Table 4.3) revealed a significant elevation in IOP in both *wt* ($p < 0.0001$) and mutant ($p = 0.003$) dogs. To investigate the transient elevation, a steroid response test was conducted with topical dexamethasone in *ADAMTS10*-mutants (n=3) and an *ADAMTS10*-carrier (n=1). An acute increase in pressure was evident within the first week of treatment (Figure 4.6). When the medications were discontinued, the pressures reverted towards baseline. Statistical analysis

Figure 4.4 IOP in *ADAMTS10*-mutant dogs injected with *AAV2(Y444F)-hADAMTS10*. Consistent with the disease phenotype, a gradual increase in pressure in both the treated and control was observed (p = 0.56). Post-injection IOPs were measured for 19 weeks.

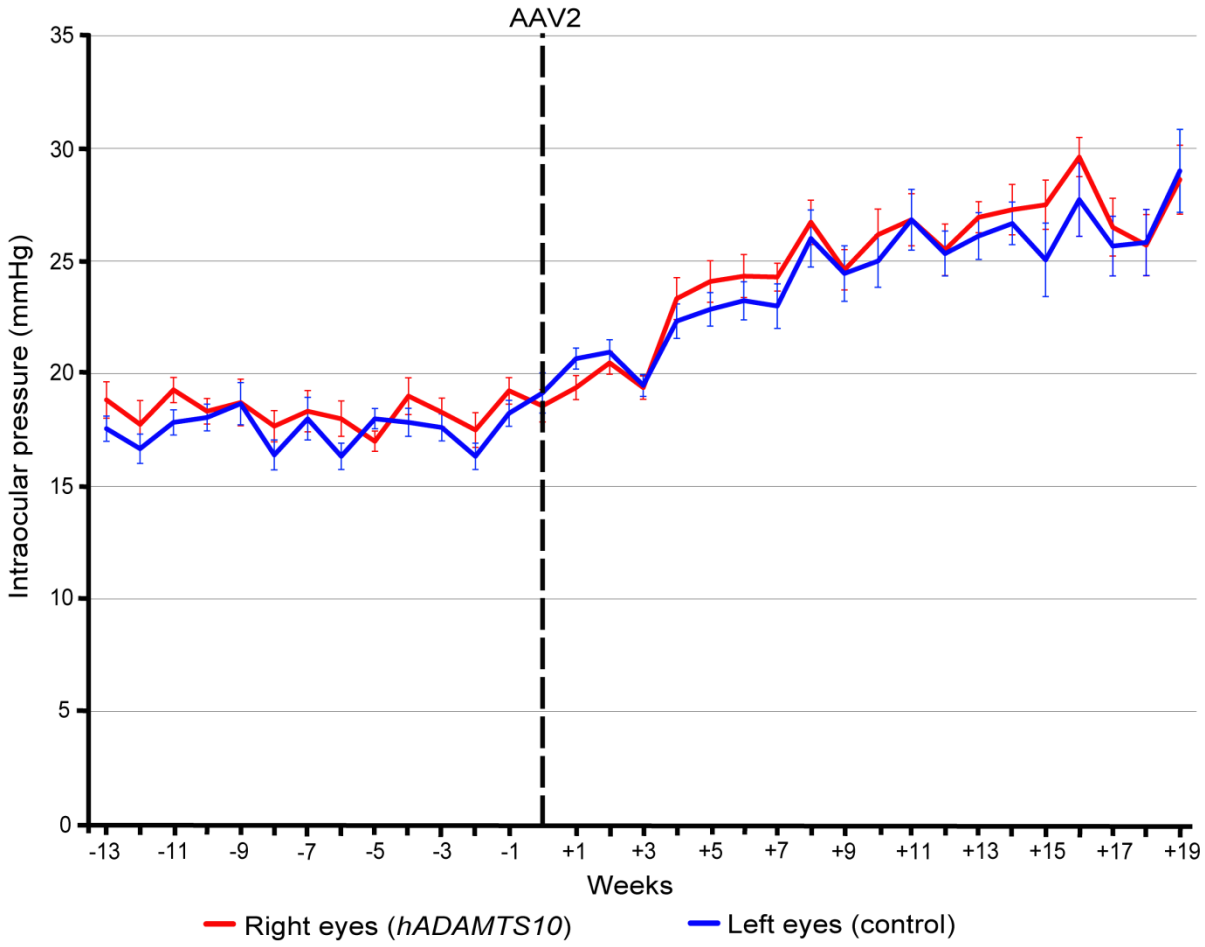

Table 4.2 Summary of excluded and abbreviated IOP data.

	AAV capsid mutant vector	Eye	Dog ID/gender	Genotype	Reasons for excluded or abbreviated IOP data	
Cohort 1	*AAV2(Y444F)-GFP*	L	5580/m	*wt*	–	Excluded data due to acute anterior chamber inflammation in the right eye (24 hours post-injection)
		L	1512/m	*wt*	–	Excluded due to a small sample size
Cohort 2	*AAV2(Y444F)-GFP*	R/L	6366/m	*ADAMTS10*- mutant	/	Abbreviated pre-injection records because subject was added later to the study
		R/L	3277/f	*ADAMTS10*- mutant	/	Abbreviated post-injection records because of a delayed onset of anterior chamber inflammation in the right eye (10 weeks post-injection)
		R/L	7930/m	*ADAMTS10*- mutant	/	Abbreviated due to a small sample size
Cohort 3	*AAV2(Y444F)-hADAMTS10*	R/L	6941/m	*ADAMTS10*- mutant	/	Abbreviated pre-injection records because subject was added later to the study; abbreviated post-injection records due to medications
		R/L	10166/f	*ADAMTS10*- mutant	–	Enrolled in the 'challenge' trial; Excluded data due to IOP-lowering medical treatment
		R/L	G19/m	*ADAMTS10*- mutant	–	Enrolled in the 'challenge' trial; Excluded data due to IOP-lowering medical treatment; Euthanized (18 weeks post-injection)
		R/L	G3/m	*ADAMTS10*- mutant	–	Euthanized (1 week post-injection)

Adeno-associated virus (AAV): AAV serotype 2 (AAV2), green fluorescent protein (GFP), *wild type* human *ADAMTS10* (*hADAMTS10*); eye: right (R), left (L), both (R/L); gender: male (m), female (f); genotype: *wild type* (*wt*), G661R variant in *ADAMTS10* (*ADAMTS10*-mutant); intraocular pressure (IOP); data: "–" excluded, "/" abbreviated.

Table 4.3 Statistics on IOP data

Cohort		*Right eye*	*Left eye*	**P-value comparing right vs left eye**
1	*Pre-injection IOP (mmHg)*	13.2± 0.31	12.9± 0.41	0.20
	Post-injection IOP (mmHg)	18.8± 0.49	18.3± 0.42	0.021
	P-value comparing pre- and post-injection IOP	< 0.0001	< 0.0001	
2	*Pre-injection IOP (mmHg)*	19.2± 1.08	18.0± 0.92	0.0005
	Post-injection IOP (mmHg)	22.8± 0.59	23.4± 0.79	0.33
	P-value comparing pre- and post-injection IOP	0.003	< 0.0001	
3	*Pre-injection IOP (mmHg)*	18.4± 0.49	17.6± 0.52	0.006
	Post-injection IOP (mmHg)	25.0± 01.03	24.4± 1.15	0.56
Cohort		*Both eyes*	**P-value**	
4	*All baseline IOPs (B)*	14.2± 0.61		
	All treatment IOPs (T)	15.6± 0.36		
	All follow up IOPs (A)	14.8± 0.28		
	B vs T		0.002	
	T vs A		<0.0001	
	B vs A		0.16	

Intraocular pressure (IOP); pre-injection IOP: before glucocorticoid treatment; post-injection IOP: during and after glucocorticoid treatment; mean± standard error.

Figure 4.5 IOP outcomes of *AAV2-GFP*. (A) In *wt* canines vector capsid mutations did affect IOP (p = 0.02) and (B) *ADAMTS10*-mutant canines, vector capsid mutations do not affect IOP since there is no significant difference (p = 0.33) in IOP between the right and left eye. The 5 mmHg increase in IOP post-AAV injection is most likely the outcome of bilateral steroid treatment (*arrows).*

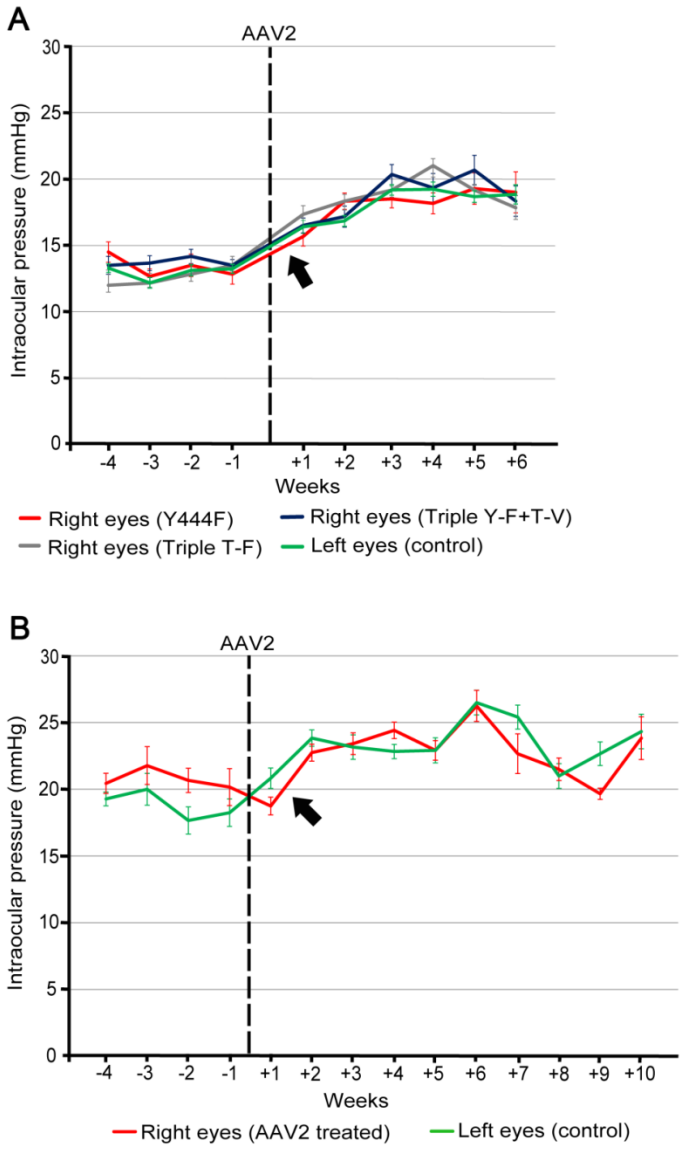

Figure 4.6 Effect of steroids on IOP in *ADAMTS10*-mutant and carrier dogs. Topical dexamethasone led to an increase in IOP within the first week of treatment. At the end of the 4-weeks, IOP immediately decreased towards baseline.

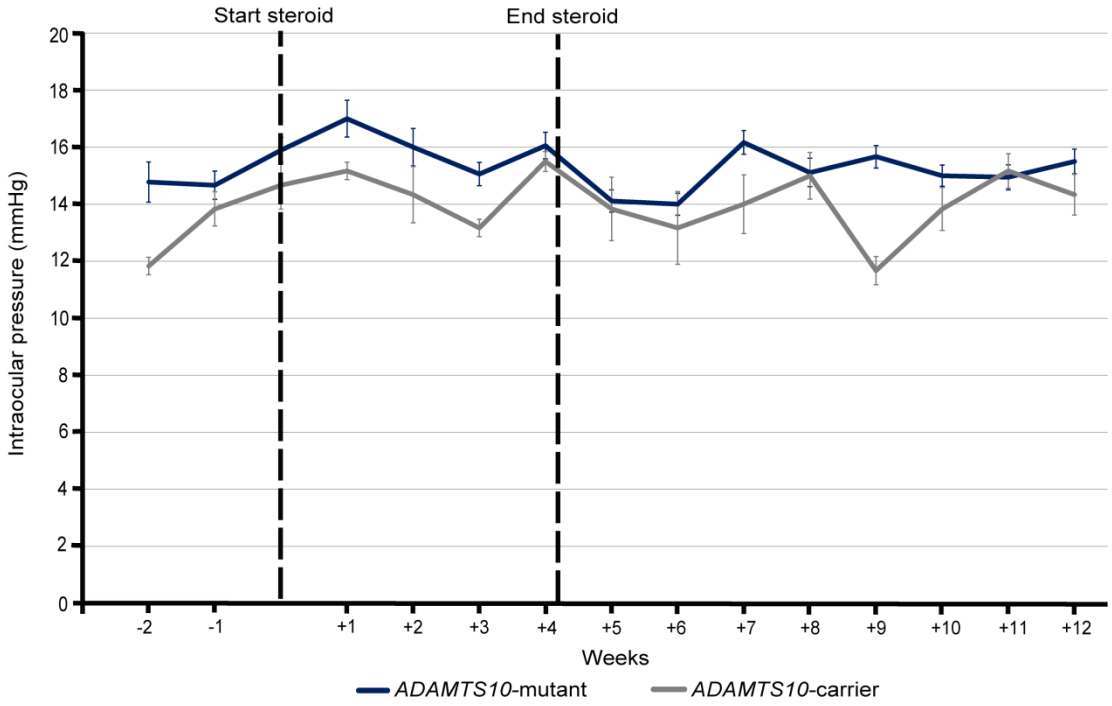

revealed a significant difference between baseline and treatment IOPs, in addition to treatment and follow-up IOPs (Table 4.3).

Clinical signs in wt and ADAMTS10-mutants

Adverse reactions were absent with the initial injections of AAV in cohort 1. The Tono-pen VET™ and Tonovet™ obtained similar pressure measurements, and a line graph of the values collected showed that AAV-based capsid mutants did not affect IOP (Figure 4.5A). Interestingly, statistical analysis (Table 4.3) revealed a marginal significant difference in pressures between injected right (18.8 ± 0.49 mmHg) and control left eyes (18.3 ± 0.42 mmHg) over 6 weeks in *wt* dogs ($p = 0.02$). The difference is too small to be clinically relevant and may be the result of a systematic measuring error introduced during tonometry (described below). The two *wt* dogs (1512 and 5580) that received the second injection of AAV2(Y444F) in the fellow eye were also monitored for 6 weeks (Table 3.1). Immediately post-injection, one of these two dogs (5580) developed mild anterior chamber inflammation and ocular hypertension, and was placed on IOP-lowering medications in addition to the already administered anti-inflammatory and anti-microbrial drugs. Even though the clinical signs quickly resolved and IOP normalized, the data for this pair were excluded from the statistics (Table 4.2). Microscopic analysis of the tissue (5580) revealed positive expression (Table 4.1)

Further adverse reactions were not observed in cohort 2 during the first 6 weeks. After two dogs were euthanized for IHC analysis, one of the remaining dogs (3277) developed moderate anterior chamber inflammation in the injected eye 10 weeks post-injection and was placed on additional medications until euthanasia. In accordance with the exclusion criterion, these data were omitted (Table 4.2). Fortunately, the complete IOP data were only abbreviated

because of the delayed onset in clinical signs. Graphical (Figure 4.5B) and statistical analysis (Table 4.3) of the injected (22.8 ± 0.59 mmHg) and control pressure (23.4 ± 0.79 mmHg) data revealed that the AAV2(Y444F) vector had no effect on IOP over 10 weeks ($p = 0.33$).

Microscopic analysis of this tissue revealed positive GFP expression in all four quadrants (Table 4.1).

Unanticipated significant differences between the right and left eyes were noted in post-injection IOPs in cohort 1 ($p = 0.02$), and pre-injection pressures in cohorts 2 ($p = 0.0005$) and 3 ($p = 0.006$; Table 4.3). Interestingly, the right eye was regularly elevated across the cohorts. In cohort 1, the outcome could have been vector related. However, since the contrast between IOP averages of the right and left eyes were so small, we suspect there was a systematic error during pressure readings. Our suspicions are further supported because IOP was consistently greater in the right eye compared to the left at most time points.

REFERENCES

REFERENCES

1. Fautsch MP, Howell KG, Vrabel AM, Charlesworth MC, Muddiman DC, Johnson DH. Primary trabecular meshwork cells incubated in human aqueous humor differ from cells incubated in serum supplements. *Investigative Ophthalmology & Visual Science* 2005;46:2848-2856.

2. Aslanidi GV, Rivers AE, Ortiz L, et al. Optimization of the capsid of recombinant adeno-associated virus 2 (AAV2) vectors: the final threshold? *PloS One* 2013;8:e59142.

3. Petrs-Silva H, Dinculescu A, Li Q, et al. Novel properties of tyrosine-mutant AAV2 vectors in the mouse retina. *Molecular Therapy: The Journal of the American Society of Gene Therapy* 2011;19:293-301.

4. Petrs-Silva H, Dinculescu A, Li Q, et al. High-efficiency transduction of the mouse retina by tyrosine-mutant AAV serotype vectors. *Molecular Therapy: The Journal of the American Society of Gene Therapy* 2009;17:463-471.

CHAPTER 5 – CONCLUSION & FUTURE STUDIES

The GFP reporter gene was successfully targeted to the canine *wt* and mutant ICA with an AAV vector. These results provided the groundwork for our chief goal of gene replacement therapy in *ADAMTS10*-mutant dogs. Canine POAG is an inherited autosomal recessive trait with an identified loss of function mutation.[1-3] Therefore, gene replacement therapy may rescue the mutant phenotype. While the intracameral administration of AAV in our studies was safe, no therapeutic effect was observed over 19 weeks at the dose evaluated. Within the treated cohort, there was no evidence of lowered IOP, or prevention of disease-related pressure spikes.

The study utilized a single-stranded recombinant AAV vector and is the first reported attempt to target gene expression to a canine ICA. We elected to administer 50 μL of vector solution at three distinct concentrations: 2×10^{10}, 2×10^{11}, and 2×10^{12} vg/mL. Efficacious targeting of the ICA was observed with the single mutant (Y444F) vector at all three concentrations; though a minimal dosing effect was noted over the viral titer range. The injection technique was effective as all four quadrants of GFP-treated eyes showed transduced TM cells. There is limited knowledge about the integrity of these cells in *ADAMTS10*-mutants dogs. Whether the TM cells are lost in the progression of the disease still remains a pertinent question, despite the marked loss observed in the ICA of human POAG eyes.[4] It also remains to be seen if transduction with the *wt* copy of the gene will result in a therapeutic effect. However the transduced cells' morphology and location suggest they are TM cells and that there is no difference between them in the *wt* and mutant dogs. To validate these results, further IHC experiments on *wt* and mutant tissue samples will be required. Since there are no specific markers for TM cells, positive and negative labeling with a combination of known antibodies

will be pursued (Table 5). Additionally, canine TM cell line cultures are currently under development. This *in vitro* model will help verify and potentially improve our technique.

Advancements in AAV-capsid based mutants have allowed us to target the ICA without the use of self-complementary vectors. Self-complementary constructs have been previously described to be the most efficient,[5] but are limited by their genomic carrying capacity. The success with conventional AAV now allows larger amounts of genetic material to be delivered to the tissue of interest. Previous studies with adenovirus in murines,[6] and lentivirus in nonhuman primates have also revealed efficacious transduction of the TM.[7] Nonetheless, AAV is the preferred viral vector in pre-clinical and clinical trials of ocular gene therapy because they produce a persistent transgene expression without eliciting a strong immune response.[8, 9] Thus, our study has provided additional evidence that AAV, specifically AAV2-capsid based mutants, can successfully target the TM.

Capsid mutant vectors have an increased nuclear translocation and transduction efficiency in the host cell because site specific mutagenesis of surface protein residues allows the vector to avoid proteasome-mediated degradation.[10] The vectors chosen for this project were based on *in vitro* and *in vivo* rodent work completed at the University of Florida, Gainesville, FL, USA.[11-13] Based on previous work we expected the triple-mutant (Y444,500,730F) and/or the quadruple-mutant (Y444,500,730F + T491V) vectors to be the most efficient. On the contrary, the vector with the single point mutation (Y444F) was the only one successful in transducing TM cells in the *wt* and mutant dogs.

Table 5.1 Positive and negative IHC markers for TM cells

Targeted antigen	Positive or negative markers	Function of antigen	References
α-smooth muscle actin	Positive	Cytoskeletal protein	[32]
Laminin	Positive	Extracellular matrix basal lamina protein	[33]
Type IV collagen	Positive	Extracellular matrix basal lamina protein	[34]
Desmin	Negative	Intermediate filament	[35]
Keratin	Negative	Intermediate filament	[36]

Administration of AAV was mostly safe at the doses chosen. The anterior chamber, vitreous cavity, and subretinal space are considered immune privileged sites and respond to antigens by diminishing the inflammatory reaction through anterior chamber associated immune deviation.[14, 15] However in a minority of dogs, rats, and monkeys, intracameral and subretinal injection of AAV vectors resulted in a clinically identifiable immune reaction.[5, 16] Readministration of viral vectors to the partner eye also has been reported to elicit an immune response.[17-20] In this study, two of the ten dogs developed mild to moderate anterior chamber inflammation after receiving an AAV carrying the GFP reporter gene. The first dog developed acute signs after vector readministration to the partner eye. Based on the onset, potential causes of inflammation include a sterile inflammatory response to the surgical procedure, acute bacterial endophthalmitis, or an immune reaction to the viral vector.[16] We hypothesize that the subject developed neutralizing antibodies from the initial injection that directly reacted with the viral vector. The second dog presented with moderate signs 10 weeks post-injection. The delayed onset suggests that an immune reaction could have developed against the transcribed GFP protein.[21, 22] Caution must be taken in future experiments as modifications to the protocol, such as increasing the vector dose, may increase the risk of side effects. Positive responses to medical treatment fortunately indicate that the inflammatory reaction may be controlled in the clinical setting.

GFP expression was rather specific along the aqueous humor outflow pathways despite the use of a non-specific promoter. A TM-specific promoter is currently not available, and thus we also observed positive cells in the anterior border and posterior pupillary margin of the iris. The tissue specificity presented in our study is unclear, and the mechanisms underlying the tissue tropisms of different AAV serotypes is not known but hypothesized to be associated with

distinctions in cellular uptake and intracellular trafficking.[23] Therefore a possible explanation is that the cells of the aqueous humor outflow pathways and anterior border of the iris express the same cell surface and co receptors allowing entry of the viral vector and subsequent intracellular trafficking. Convection currents present in the anterior chamber due to thermal circulation[24] may also contribute by widely distributing the vector and prolonging the vector-host cell interaction before it exits through the ICA. Interestingly, inner corneal cells were not transduced. Furthermore, since all aqueous humor is drained through and filtered by the TM, this may 'concentrate' the AAV-mediated gene expression to the outflow pathways. As mentioned previously, further characterization of the transduced cells is necessary.

Even though the expression of GFP in the ICA was present on microscopy, we did not observe *in vivo* expression by gonioscopy. This infers that the fluorescence was less prominent in our dogs compared to previous studies in other species.[5, 7] Examination with confocal microscopy revealed that relatively few TM cells fluoresced while other surrounding cells were GFP-negative. The BLAST identity between hADAMTS10 and cADAMTS10 protein was 96%, suggesting the *wt* human transgene product could function as a substitute in *ADAMTS10*-mutant dogs.[25] Thus, a low transgene expression may possibly explain the lack of therapeutic effect seen with *AAV2(Y444F)-hADAMTS10*. The goal of future trials would then be to increase the number of TM cells transduced by modifying procedural strategies such as increasing the vector solution volume, or using higher viral titers (10^{13} vg/mL). Unfortunately, the latter would be difficult since our highest concentration was already stock solution from University of Florida. Additional approaches would be to substitute the steroid therapy with NSAIDs to eliminate dexamethasone's confounding effect on IOP, or to enroll a younger cohort of dogs (< 8 weeks of age) to target the ICA during its final stages of development and/or much earlier before the onset

of the POAG phenotype. Furthermore, atropine could be used to temporarily decrease the aqueous humor outflow through the ICA to prolong AAV contact time. Quantitative measures of transduction efficiency, including qRT-PCR (mRNA) and Western blot/IHC (protein) of GFP and hADAMTS10, will be pursued in the future once the 6-month post-injection observation period has been concluded.

Initial trials with presumed therapeutic *AAV2(Y444F)-hADAMTS10* vector did not show any effect over 19 weeks. We treated both pre-glaucomatous and glaucomatous mutant dogs, and the results showed progressive bilateral increase in IOP over time (Figure 4.4) and sustained IOP > 40 mm Hg, respectively. Based on the GFP study we assume that the *wt* hADAMTS10 protein was expressed, but the lack of therapeutic effect suggests that a larger number of transduced TM cells and subsequently transcribed proteins may be required to augment the phenotype. The presence of hADAMTS10 protein in the treated eyes still needs to be confirmed by Western blot, IHC of ocular tissue, and ELISA of aqueous humor, in addition to qRT-PCR of extracted RNA. We also hypothesize that more time is needed for the accumulated ECM to be removed when the *wt* ADAMTS10 re-establishes microfibril homeostasis. Therefore the decision has been made to continue monitoring the IOP of the treated cohort up to 6 months post-injection. Once future gene therapy trials have been shown to be successful, we will specifically look at the 'timing' of excessive ECM material removal. We also want to collect additional quantitative measurements of conventional aqueous humor outflow by pneumatonography to support the IOP data. Furthermore, we unexpectedly observed significant distinctions between the right and left eye in baseline IOPs of cohorts 2 and 3, as well as follow-up pressures in cohort 1. IOP could be slighted elevated in one eye even though the disease progresses bilaterally.[1] However previous studies have reported no statistical difference when

comparing left and right eyes in normal dogs,[26] and thus it is unusual that the right eye was regularly elevated across the cohorts. For that reason, we hypothesize that a systematic error may have occurred during pressure reading, and the hand/tonometry positioning and/or animal handling may have affected pressure measurements.

Glucocorticoids are the likely culprit for the transient increase in IOP observed following AAV administration to both treated and controls eyes as steroids were used in this study in order to decrease the risk of vector-induced uveitis. Glucocorticoid-induced ocular hypertension is a well-known phenomenon and has been described in several species including humans[27], rabbits[28], cats[29], cows[30], and most recently sheep[31]. A former study in glaucomatous dogs treated with topical 0.1% dexamethasone revealed a reversible ~5 mm Hg increase in IOP.[32] To the best of our knowledge this is the first documented report of dexamethasone-induced ocular hypertension in *wt* dogs. There is only one other study that unexpectedly observed ocular hypertension in a heterogeneous group of dogs with cataracts treated one-week preoperatively with topical 1% prednisolone acetate.[33] On the contrary, oral hydrocortisone administration for 5 weeks did not elevate IOP in clinically normal dogs[34] In order to verify the effect of dexamethasone in our cohorts, we performed a small trial and found significantly higher IOPs recorded for both the mutant and carrier dogs during the first week of the 4-week treatment. However compared to cohorts 1 and 2, the increase was not as great and long-lasting. We hypothesize that there may be a difference between the effects of oral and topical glucocorticoids. In future studies, a larger sample size should be used to evaluate the influence of steroid delivery on IOP.

In conclusion, conventional AAV2 with capsid mutations transduced the TM in *wt* and *ADAMTS10*-mutant dogs. The dose implemented in this study was reasonably safe, and

consistent GFP expression was detected in the aqueous humor outflow pathways and anterior border of the iris. A therapeutic effect has not yet been observed however upcoming experiments have been planned to verify and improve our knowledge of the presented outcomes. Familial aggregation is still a major risk factor in the development of human POAG, and current and future projects continue to uncover genes linked to the pathogenesis of the disease. Therefore phenotypic characterization and therapy trials in spontaneous animal models continue to offer exceptional opportunities for proof-of-principle experiments. The results reported here have provided a solid foundation for successful TM-directed gene therapy.

REFERENCES

REFERENCES

1. Gelatt KN, Gum GG, Gwin RM, Bromberg NM, Merideth RE, Samuelson DA. Primary open angle glaucoma: inherited primary open angle glaucoma in the beagle. *The American Journal of Pathology* 1981;102:292-295.

2. Kuchtey J, Olson LM, Rinkoski T, et al. Mapping of the disease locus and identification of ADAMTS10 as a candidate gene in a canine model of primary open angle glaucoma. *PLoS Genetics* 2011;7:e1001306.

3. Kuchtey J, Kunkel J, Esson D, et al. Screening ADAMTS10 in dog populations supports Gly661Arg as the glaucoma-causing variant in beagles. *Investigative Ophthalmology & Visual Science* 2013;54:1881-1886.

4. Tektas OY, Lutjen-Drecoll E. Structural changes of the trabecular meshwork in different kinds of glaucoma. *Experimental Eye Research* 2009;88:769-775.

5. Buie LK, Rasmussen CA, Porterfield EC, et al. Self-complementary AAV virus (scAAV) safe and long-term gene transfer in the trabecular meshwork of living rats and monkeys. *Investigative Ophthalmology & Visual Science* 2010;51:236-248.

6. Budenz DL, Bennett J, Alonso L, Maguire A. In vivo gene transfer into murine corneal endothelial and trabecular meshwork cells. *Investigative Ophthalmology & Visual Science* 1995;36:2211-2215.

7. Barraza RA, Rasmussen CA, Loewen N, et al. Prolonged transgene expression with lentiviral vectors in the aqueous humor outflow pathway of nonhuman primates. *Human Gene Therapy* 2009;20:191-200.

8. Buning H, Perabo L, Coutelle O, Quadt-Humme S, Hallek M. Recent developments in adeno-associated virus vector technology. *The Journal of Gene Medicine* 2008;10:717-733.

9. Flotte TR, Carter BJ. Adeno-associated virus vectors for gene therapy. *Gene Therapy* 1995;2:357-362.

10. Zhong L, Li B, Mah CS, et al. Next generation of adeno-associated virus 2 vectors: point mutations in tyrosines lead to high-efficiency transduction at lower doses. *Proceedings of the National Academy of Sciences of the United States of America* 2008;105:7827-7832.

11. Aslanidi GV, Rivers AE, Ortiz L, et al. Optimization of the capsid of recombinant adeno-associated virus 2 (AAV2) vectors: the final threshold? *PloS One* 2013;8:e59142.

12. Petrs-Silva H, Dinculescu A, Li Q, et al. Novel properties of tyrosine-mutant AAV2 vectors in the mouse retina. *Molecular Therapy: The Journal of the American Society of Gene Therapy* 2011;19:293-301.

13. Petrs-Silva H, Dinculescu A, Li Q, et al. High-efficiency transduction of the mouse retina by tyrosine-mutant AAV serotype vectors. *Molecular Therapy: The Journal of the American Society of Gene Therapy* 2009;17:463-471.

14. Streilein JW. Ocular immune privilege: therapeutic opportunities from an experiment of nature. *Nature Reviews Immunology* 2003;3:879-889.

15. Willett K, Bennett J. Immunology of AAV-Mediated Gene Transfer in the Eye. *Frontiers in Immunology* 2013;4:261.

16. Bainbridge JW, Mistry A, Schlichtenbrede FC, et al. Stable rAAV-mediated transduction of rod and cone photoreceptors in the canine retina. *Gene Therapy* 2003;10:1336-1344.

17. Bennett J, Ashtari M, Wellman J, et al. AAV2 gene therapy readministration in three adults with congenital blindness. *Science Translational Medicine* 2012;4:120ra115.

18. Hauswirth WW, Aleman TS, Kaushal S, et al. Treatment of leber congenital amaurosis due to RPE65 mutations by ocular subretinal injection of adeno-associated virus gene vector: short-term results of a phase I trial. *Human Gene Therapy* 2008;19:979-990.

19. Amado D, Mingozzi F, Hui D, et al. Safety and efficacy of subretinal readministration of a viral vector in large animals to treat congenital blindness. *Science Translational Medicine* 2010;2:21ra16.

20. Annear MJ, Bartoe JT, Barker SE, et al. Gene therapy in the second eye of RPE65-deficient dogs improves retinal function. *Gene Therapy* 2011;18:53-61.

21. Guziewicz KE, Zangerl B, Komaromy AM, et al. Recombinant AAV-mediated BEST1 transfer to the retinal pigment epithelium: analysis of serotype-dependent retinal effects. *PloS One* 2013;8:e75666.

22. Beltran WA, Boye SL, Boye SE, et al. rAAV2/5 gene-targeting to rods:dose-dependent efficiency and complications associated with different promoters. *Gene Therapy* 2010;17:1162-1174.

23. Wu Z, Asokan A, Samulski RJ. Adeno-associated virus serotypes: vector toolkit for human gene therapy. *Molecular Therapy: The Journal of the American Society of Gene Therapy* 2006;14:316-327.

24. Gelatt KN, Gilger BC, Kern TJ. *Veterinary Ophthalmology*. 5th ed. Ames, Iowa: Wiley-Blackwell; 2013.

25. Altschul SF, Gish W, Miller W, et al. Basic local alignment search tool. *Journal of Molecular Biology* 1990;215:403-410.

26. Giannetto C, Piccione G, Giudice E. Daytime profile of the intraocular pressure and tear production in normal dog. *Veterinary Ophthalmology* 2009;12:302-305.

27. Kersey JP, Broadway DC. Corticosteroid-induced glaucoma: a review of the literature. *Eye* 2006;20:407-416.

28. Ticho U, Lahav M, Berkowitz S, Yoffe P. Ocular changes in rabbits with corticosteroid-induced ocular hypertension. *The British Journal of Ophthalmology* 1979;63:646-650.

29. Zhan GL, Miranda OC, Bito LZ. Steroid glaucoma: corticosteroid-induced ocular hypertension in cats. *Experimental Eye Research* 1992;54:211-218.

30. Gerometta R, Podos SM, Candia OA, et al. Steroid-induced ocular hypertension in normal cattle. *Archives of Ophthalmology* 2004;122:1492-1497.

31. Gerometta R, Podos SM, Danias J, Candia OA. Steroid-induced ocular hypertension in normal sheep. *Investigative Ophthalmology & Visual Science* 2009;50:669-673.

32. Gelatt KN, Mackay EO. The ocular hypertensive effects of topical 0.1% dexamethasone in beagles with inherited glaucoma. *Journal of Ocular Pharmacology and Therapeutics: The Official Journal of the Association for Ocular Pharmacology and Therapeutics* 1998;14:57-66.

33. McLean NJ, Ward DA, Hendrix DV, Vaughn RK. Effects of one-week versus one-day preoperative treatment with topical 1% prednisolone acetate in dogs undergoing phacoemulsification. *Journal of the American Veterinary Medical Association* 2012;240:563-569.

34. Herring IP, Herring ES, Ward DL. Effect of orally administered hydrocortisone on intraocular pressure in nonglaucomatous dogs. *Veterinary Ophthalmology* 2004;7:381-384.